A PHYSIOLOGICAL SENSOR NETWORK SUPPORTED BY AN INDUCTIVE COMMUNICATION LINK

by

SETH HOSKINS

B.S., KANSAS STATE UNIVERSITY, 2006

A THESIS

submitted in partial fulfillment of the

requirements for the degree

MASTER OF SCIENCE

Department of Electrical & Computer Engineering

College of Engineering

KANSAS STATE UNIVERSITY

Manhattan, Kansas

2011

Approved by

Major Professor

Steve Warren

ABSTRACT

The continuous and autonomous real-time monitoring of cattle state of health can provide major benefits for the U.S. livestock industry and lead to a higher quality beef product. Complete real-time monitoring could not only lead to earlier detection of disease in individual animals and reduce the spread of disease to a larger herd, but it could ultimately reduce the cost and frequency of on-site veterinary consultations.

This thesis details a wearable device that is mounted on cattle to collect data from a network of internal and external sensors. In addition to the basic data collection, this thesis will describe the infrastructure to communicate these data sets to a central database for permanent storage and future analysis. Physiological, ambient environment, and physical activity data are acquired by the various sensors to give a good indication of the state of health of an animal wearing the device.

The communication of data from internal sensors to an external wearable receiver is of particular interest since tissue is not an ideal medium for radio-frequency data transmission. Past research has attempted to use such links with little success due to large signal attenuation at high frequencies and a package that becomes much too large to be usable at low frequencies. As a result, a wireless communications method employing magnetic inductance at relatively low frequencies over short distances is described here.

TABLE OF CONTENTS

LIST OF FIGURES

ACKNOWLEDGMENTS

This author would like to acknowledge the collaborators, students, and professors who helped make this thesis possible. First, I would like to thank my major professor, Dr. Steven Warren, KSU Electrical & Computer Engineering, for the ideas, laboratory space, and technology he has provided, in addition to supplying editing feedback and overall project direction. Next, I would like to thank Timothy Sobering and his colleagues at the KSU Electronics Design Laboratory for providing technical assistance and design advice. I also wish to thank Dr. Daniel Andresen, KSU Computing & Information Sciences, for his input and for the invaluable assistance he and his students have provided during the project. I also wish to thank Dr. William Kuhn, KSU Electrical & Computer Engineering, for providing insight into antenna design and pointing me toward the instrumentation needed to help test and tune my circuits. I would also like to thank Dr. Tammi Epp and Dr. Howard Erickson, KSU Anatomy & Physiology, KSU College of Veterinary Medicine, for their assistance in gaining access to research animals and for their insight into cattle health assessment. Tammi was a particular asset because of her assistance with the handling of animals during research. I would like to thank all of the other student collaborators on the BMOO project, both past and present, whose research has provided the building blocks of this thesis and whose efforts will move this project forward. Finally, I want to send a big thanks to all of my friends and family who have been there to support me over the years.

CHAPTER 1: INTRODUCTION

The American livestock industry represents the largest single contributor to the American agricultural economy [1]. The average American consumer will spend $249 on beef per year and consume 59.9 pounds of beef, where hamburger and steak represent the most popular menu items at many American restaurants. Due in part to recent disease outbreaks, massive beef recalls, and a rising health consciousness, many consumers seek beef solely from the healthiest animals available. This is evident in the fact that the fastest growing portion of the beef industry comes from natural beef which consists of antibiotic free, hormone free animals that have been fed purely organic vegetables.

While it is unreasonable for all cattle ranches to produce only natural beef, better animal tracking and health monitoring could increase the average quality of the beef supply and the health of the average American. In addition to providing a better product, tracking and monitoring is vital in protecting livestock from disease whether from natural causes or bioterrorism. With this continual monitoring, disease could be detected earlier than with sparse visual checks of animals, thus infected animals could be quarantined from the larger herd. This would not only hinder disease spread, but could eventually lessen antibiotic use with healthy animals.

The United States Department of Agriculture (USDA) has already initiated a country wide tracking system, the National Animal Identification System (NAIS), to track a large segment of the livestock population including cattle, chickens, pigs, horses, sheep, and other animals [2]. However, this system is designed only to track and prevent disease spread in animals that are being moved around and co-mingle with larger populations. This system has no provisions for the health monitoring of individual animals to detect the onset of disease; it is only a method to track and limit disease.

Long-term health monitoring of individual cattle may prove burdensome because there are multiple metrics to be considered and few available methods for continuous measurement of these values. Heart rate, respiration rate, and core body temperature

stand out as three of the most crucial indicators of state of health, and there is a vast amount of clinical information defining healthy and unhealthy thresholds for each. Heart rate can be collected over time, and deviations from each animal's mean value can indicate changes in state of health and stress levels. Respiration rate can also be an indication of general health since many diseases cause respiratory disorders. Core body temperature has been shown to provide information relating to an animal's drinking and eating habits as well as its rumination cycles.

Separate commercial packages have been developed to measure heart rate, core body temperature, and respiration rate. Heart rate measurement devices usually come in a belt-based arrangement but are only meant to be used for short periods of time. These belts often require significant maintenance since a gel or paste needs to be applied periodically to ensure optimal contact between the external electrode and an animal's hide. The belts are also not feasible for continuous use because they are not made to endure harsh outdoor conditions and often require a clinical technician to monitor the animal to guarantee the belt is not loosened or broken. Subdermal electrodes that do not require a belt also exist, but these may require minor surgery on each animal and can result in infection and further stress to the animal. Respiration rate is commonly measured with pressure sensors that detect changes in thoracic volume, but it can also be deduced from phonocardiograms and electrocardiograms. Core temperature measurement devices exist in the form of a pill whose battery life can span months once swallowed by an animal. However, this provides a single metric, and it would be much more efficient to package a pill sensor that acquires more than one vital parameter.

However, transmitting data from the inside of a large animal to the outside offers its own hurdles. Traditional wireless transmission relies on radio waves to propagate from a source to a destination. This form of transmission is well suited for an air medium but does not perform as well in a biological or water-based medium. This is because the high frequency signals attenuate to the point that they do not reach their destination. Lower frequencies tend to work better, but to efficiently transmit at low frequencies, a very large antenna is needed that is not suited for internal placement.

These factors indicate the necessity for a less traditional form of wireless transmission that is not greatly affected by the transmission medium. One alternative exists in the form of wireless transmission via magnetic inductance, which has its own set of advantages and disadvantages. On the positive side, magnetic links consume less power, require fewer components, are not affected by the transmission medium, and are physically smaller when compared to traditional radio links. On the negative side, magnetic inductive links are affected by antenna orientation, do not have as much transmission range, and transmit weaker signals when compared to traditional radio links.

This thesis details a prototype sensor network designed for livestock that monitors a range of external and internal stimuli to characterize state of health. Along with the individual sensors, the document will also explore the wearable device that aggregates data until they can be transmitted to a PC for permanent storage. Next, it will address the design of a magnetic inductive link to transmit data from internal sensors to an external wearable device. Finally, it will explore the internal sensor device under development meant to directly detect internal heart rate, core body temperature, and respiration rate.

CHAPTER 2: BACKGROUND

The Kansas State University (KSU) Electrical and Computer Engineering Department, in collaboration with the KSU Department of Computing and Information Sciences and the KSU College of Veterinary Medicine have resources in the KSU Medical Component Design Laboratory to design monitoring platforms that address the issue of long term cattle tracking and health assessment. The prototype system has been referred to as the Bovine Mobile Observation Operation (BMOO). This collaborative group, funded by a grant from the National Science Foundation Information Technology Research Program (ITR–0325921 and ITR–0205487), has developed a prototype wearable unit with continuous external sensors, temporary data storage, and a means to wirelessly transmit the data to a PC where they can be permanently stored in a database for retrieval and analysis. The group has also begun development on a method of wireless transmission based on magnetic inductance to transmit data from within an animal to an external wearable device. The magnetic inductive link will eventually be applied to a sensor pill or bolus, also in development, which measures a bovine's heart rate, respiration rate, and core body temperature internally.

A number of graduate students and faculty have contributed to the BMOO project to get it to this point. Much of the initial design of the wearable unit, nicknamed the BMOO unit, was performed by Luke Nagl, who designed the majority of the hardware and the early software [3]. Dominic Gelinas later updated the software to include object-oriented design via C++ elements and structures [4]. They began with proof of concept prototypes to aggregate data from an array of sensors. With guidance from Tammi Epp and Howard Erickson (KSU College of Veterinary Medicine), the team defined the initial data to collect: three axis acceleration, global positioning (GPS), ambient temperature and humidity, heart rate, and core body temperature. Physical activity could potentially be monitored by measuring all three axis of acceleration. This was accomplished by orthogonally arranging a pair of two-axis ADXL accelerometers manufactured by Analog Devices [5]. A Garmin GPS-16L unit was initially used for GPS, but this was large, expensive, and consumed a lot of power. A cheaper, smaller alternative, the Trimble

Lassen SQ GPS unit [6], has been implemented in current prototypes, although the system remains flexible enough to allow for changes in future revisions.

The early system measured core body temperature and heart rate with commercial packages. In early trials, core body temperature was assessed using a subcutaneous implant system manufactured by Digital Angel. While Digital Angel's implant provided temperature and a basic animal RFID system, the implant required an injection and it was not deep enough to constitute true core temperature. While the infrastructure still exists to support this subsystem, as of the latest revision it has not been tested and is not directly supported. Instead, to measure true core body temperature, a CorTemp sensor pill [7] manufactured by HQI, Inc is employed. It communicates wirelessly with a reader unit, which then communicates with a wearable device via an RS-232 serial communications link. A belt manufactured by Polar, Inc, originally used on horses, was used to get heart rate data. The same HQI data reader device (a research unit designed by HQI) was used to relay data to the BMOO unit.

Luke Nagl also began initial testing of a wireless communication method to get the data from the BMOO unit to a computer database where the data could be stored permanently. Originally he used a Bluetooth system that employed a PDA as a base station, but due to expense, power draw, and overly complicated implementation, Bluetooth was abandoned for an emerging low power wireless protocol known as Zigbee [8]. This project started using the Microchip Zigbee implementation very early in its development cycle when numerous bugs existed, but Dominic Gelinas and Kevin Smith managed to get a rudimentary communications to work intermittently. Since that time, Dan Wilson and I have achieved a working communications system between the BMOO Unit and a base station connected to a laptop. Chapter 3 further details the current system including the complete BMOO unit as well as the wireless communication system currently implemented.

Efforts on an ingestible BMOO bolus were started with a device designed by Scott Schoenig to monitor heart rate and core temperature. This initial version relied on

acoustic sensors to obtain a phonocardiograph which could ideally be used with peak detection circuitry to obtain the heart rate. This approach was later supplemented with piezoelectric sensors that could measure heart rate via transduction of these pressure waves and an analog low-voltage temperature sensor. Heart rate measurement via a phonocardiogram was a unique approach, as it recorded the analog sounds inside an animal and used digital peak detection algorithms to determine heart beat cycles and to potentially construct a phonocardiogram profile. While this proved sporadically successful, the internal background noise (e.g., from rumenation) would often overpower the heart sounds. However, complete suppression of these superfluous noises may prove counterproductive in overall health assessment because these sounds could potentially reveal information about rumination cycles. Angel Martinez along with Tim Sobering continued development of the ingestible pill and combined the acoustic technique with electrocardiographic and piezoelectronic techniques.

Although a prototype bolus was developed, there still was no way to wirelessly transmit the data from the pill to the external BMOO unit. Up to this point, testing has only been done with wired pills in fistulated steers, where cannulas allow direct access to the rumen and reticulum of these animals. Patrick York began work on a magnetic inductive wireless link based on a MicroChip design (AN-232) [9]. This design worked in free space and with saline immersion tests, but it relied on larger than desired, custom air core antennas. Chapter 4 details this design and the efforts to continue this work.

While trials have been done on single animals thus far, the eventual goal is to support entire herds and further develop human interfaces such that any animal's state of health can be perceived with a brief glance. It would also be such that advanced software algorithms could be applied to the data in near real-time to alert owners to recognized health concerns, so that uninterrupted manual monitoring is not essential.

CHAPTER 3: BMOO UNIT

A. Overview

The BMOO (Bovine Mobile Observation Operation) unit is the unofficial name given to the wearable bovine monitoring device developed by the collaborators on this effort. The unit consists of a network of sensors that measure physiologic activity and environmental data, supported by a data logger that temporarily stores and eventually sends data wirelessly to a base station that attaches to a server for permanent data storage. Each unit is mounted in a housing which protects it from damage, and it is placed in a harness fitted around the thorax of a bovine. The data logger is powered by a 6 V DC battery which also provides power to the sensors. A TERN Flashcore-B microcontroller [10] is the central component of the data logger, where all collected sensor data are temporarily stored on a CompactFlash [11] memory card. In addition to its data aggregation functions, the TERN transfers sensor data to the BMOO unit's secondary PIC 18F2620 microcontroller [12] commissioned with the task of wireless communication. The secondary microcontroller employs ZigBee software and radio hardware [13] to relay the data to a physically separate, PC-connected base station for permanent storage. Figure 1 shows the system block diagram in terms of the sensors, data logger, and base station. A full hardware schematic is contained in Appendix A.

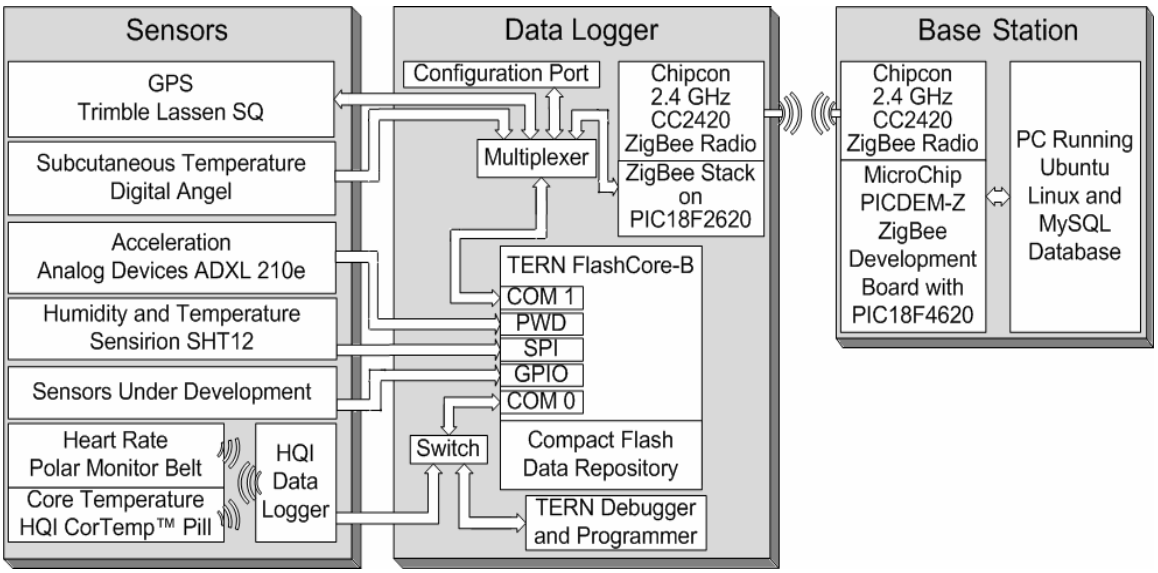

Figure 1. BMOO system block diagram.

B. TERN FlashCore-B

A TERN FlashCore-B (FCB) [10] is the primary microcontroller on the BMOO unit. It controls the sensor data flow by reading the sensors, temporarily storing these data, and then forwarding them to a secondary microcontroller which manages the wireless communications. This microcontroller was originally chosen because of its high-speed, built-in CompactFlash (CF) interface, flexibility due to numerous input/output (I/O) pins, power regulation, and inclusion of a complete software programming package with C/C++ support.

The FCB processor is a 16-bit 80186 derivative which can operate at two clock frequencies: 20 MHz or 40 MHz. Unlike numerous other microcontrollers, it operates at the true listed frequency without internal clock divisions, so the 40 MHz mode can truly achieve 40 million instructions per second. The BMOO unit utilizes the 20 MHz option because this yields ample time to service all of the sensors while also achieving longer battery life than the 40 MHz option. The FCB includes a precise Dallas Semiconductor DS1337 [14] real-time clock that allows sensor data to be time stamped. The DS1337 provides time resolutions from years down to tenths of a millisecond and is backed up by a 5 V lithium ion coin battery, ensuring timing accuracy for up to five years without the application of an external power source.

When the BMOO unit was originally designed, the CF nonvolatile mass storage format was one of the most widespread portable storage formats, providing significant storage capacity in a small enclosure [11]. While physically smaller and faster storage formats with more capacity have been developed since the project began (e.g., SMART Media and MicroSD), CF still suits the needs of the BMOO unit and the current application, supporting file systems of up to one gigabyte: enough storage for up to a week of continuous sensor data. The FCB not only provides software libraries to support a

number of file systems, but its battery backup system also keeps track of segments written to flash memory in order to avoid corruption in case of inadvertent power failure.

The FCB has two direct memory access (DMA) serial communication ports (COM ports) that each support 8-bit or 9-bit communication up to 57,600 bps using its RS232 drivers in the 20 MHz mode. It also contains three 16-bit timers, two of which can be used for pulse width modulation (PWM) or demodulation (PWD), and a supplemental watchdog timer supported by a MAX691 on-board supervisor chip [15] that ensures proper software execution and detects power failure. The PWD feature is atypical of most microprocessors, but it is a practical feature for the BMOO unit since PWD provides the ability to efficiently measure a signal's high versus low phases via hardware, thus enabling the FCB to rapidly decipher incoming PWM signals. In addition to these features, the FCB has six external interrupt inputs and 32 additional versatile programmable I/O pins that can act as general purpose input/output pins (GPIO) or implement serial protocols such as Serial Peripheral Interface (SPI), Inter-Integrated Circuit (I^2C), Controller Area Network (CAN), or any number of customized protocols.

Additionally, the FCB is packaged with a Texas Instruments TPS76550 5V low-dropout (LDO) voltage regulator [16], making it ideal for use with unstable power sources such as batteries. Not only is the FCB's on-board regulator used for the FCB itself, but it is also used as a supply for some of the support hardware on the BMOO unit. Most notably, it reliably powers serial line multiplexers that allow multiple sources to communicate with the FCB over a single communications port.

Finally, the Paradigm integrated development environment (IDE) for embedded C/C++ [17] is provided with the FCP. The Paradigm software includes a compiler and debugger that require nothing more than a simple serial cable as opposed to a hardware compiler many microcontroller devices need. While one of the FCB's serial communications ports is required for programming and debugging the microprocessor, once a user program is put into FCB memory, the program can flag the port to be used for other purposes by changing some register values. Taking advantage of this, a simple hardware switch was

added to the BMOO unit to allow the user to put the FCB into either a programming mode or a data mode where data from an external data logger developed by HQI are forwarded to the BMOO data logger. The FCB also handles user interaction with the BMOO unit through a configuration port that connects a PC to the serial port and offers a text based user interface. This allows a user to assign each BMOO unit a unique identification number, format a new CF media card with the basic BMOO file system, or perform a cold start on the GPS unit, which properly configures the GPS output string format and initiates satellite acquisition.

C. Sensor Network

The BMOO unit's network of sensors is designed to continuously track cattle location, measure physical activity, and monitor physiologic data. The flow of data from this network converges at a BMOO unit's FCB, which continuously polls each sensor at the appropriate sampling interval. When the time arrives for a particular sensor to be polled, an FCB attempts to collect data; if it is successful, the data are organized into packets that are temporarily stored on the FCB's CF. Currently, the network includes sensors to measure global position, three-axis acceleration, ambient temperature, ambient humidity, heart rate, and core body temperature.

C.1 Global Position

Cattle tracking is provided by way of GPS location data using a Trimble Lassen SQ GPS receiver [6], which includes a small antenna and a larger processing unit. The device communicates with the FCB over an RS-232 COM port. However, due to the two COM-port limitation of the FCB, the GPS shares a communication bus with the user's configuration port, a Digital Angel line, and the ZigBee enabled microcontroller (see section C.5). The bus is made possible by a separate hardware multiplexer that is controlled by two of the FCB's general purpose I/O (GPIO) pins.

The GPS module has two basic modes of operation. The first is based on the Trimble Standard Interface Protocol (TSIP) [18], and the second is based on the National Marine Electronics Association 0183 (NMEA) protocol [19]. The TSIP is a bidirectional

standard developed by the GPS manufacturer that allows flexibility in the module and provides the ability to interact with a range of PC programs provided by Trimble. The NMEA protocol is a well established, output-only industry standard that defines the data format and COM port interface for GPS messages. The BMOO unit makes use of both of these protocols but typically uses TSIP to configure the GPS module and NMEA to receive GPS location data.

The TSIP mode runs at 9600 baud with 8 data bits, odd parity, 1 stop bit, and no flow control, and it allows a user to send command packets to the GPS module. Command packets follow the structure: <DLE> <ID> <data string> <DLE> <ETX>, where DLE and ETX are ASCII characters with the respective hexadecimal values of 0x10 and 0x03. ID is a one-byte command identification value, and the data string is the payload for the command specified by ID. These command packets fall into two basic categories: query packets and configuration packets. Query packets sent to the GPS module generate a response – a report packet whose content depends on the query ID and data string. Report packets follow the same basic structure as command packets, but they contain a different output ID and payload that can contain information such as satellite tracking information or current setup parameters. Configuration packets again follow the TSIP structure but are used to assign parameter values (such as current position), initiate specific actions (such as reset), or configure the automatic output mode.

The module can operate in two modes (query mode and automatic mode), although query mode is primarily utilized by the BMOO unit during TSIP interaction. In query mode, the module responds with report packets, but in automatic mode the module constantly sends GPS location information at fixed intervals. The output information in automatic mode can be configured by the user, but the BMOO unit does not rely on TSIP for GPS location information. Rather it uses the more widely recognized NMEA standard.

The NMEA mode runs at 4800 baud with 8 data bits, no parity, 1 stop bit, and no flow control. The BMOO implementation of NMEA acquires the recommended minimum navigational information (MNI) [19], which includes date, time, latitude, latitude

direction, longitude, longitude direction, speed, tracking, magnetic variation, and magnetic variation direction. These data are transmitted from the GPS module in a comma-delimited ASCII string beginning with $GPRMC to indicate the start of a GPS minimum content message. Latitude and longitude are both six characters: two for degrees, two for minutes, and two for fractions of a minute, while direction is a single character (N, S, E, or W). Time is eight characters: two for hours, two for minutes, two for seconds, and two for fractions of a second. Date is six characters: two for days, two for months, and two for years. Speed over ground is measured in knots and is a six character string. Tracking and magnetic variation are both variable-length values measured in degrees and can incorporate fractions of a degree. Once a string is received, the ASCII text is converted into the respective integers, which are then stored on CF media.

C.2 Three-Axis Acceleration

Acceleration supplied to the BMOO unit is not simply the forward velocity shift normally associated with acceleration, but rather a three-axis measure of *g*-force, both drastic and subtle (in this case head movement). This sensor allows the BMOO unit to quantify movements that are impossible for GPS to detect in an effort to categorize the physical activity of an animal. Overall physical activity level is an important indicator of health because sick animals often appear more lethargic in comparison to their healthier counterparts. Additionally, assessments of particular animal behaviors have the potential to yield indicators for animal heath and well-being that have not been previously investigated. Raw acceleration data are problematical to interpret visually, so work within the BMOO group has been done to use artificial intelligence (AI) algorithms to correlate raw accelerometer data to the specific common behaviors [20].

A three dimensional acceleration vector is provided for the BMOO unit by orthogonally arranging a pair of two-axis ADXL210E accelerometers [5] and disregarding one of the overlapping axes. Each accelerometer axis reports both static and dynamic acceleration by outputting a PWM signal whose duty cycle is proportional to acceleration over the full-scale range of ±10 *g*. The frequency range of each accelerometer is set using a pair

of identical capacitors that form a low-pass filter. This range is set to 50 Hz with a 0.1 µF capacitor providing a resolution of $7.2*10^{-3}$ *g*. The FCB then is ideal for reading data from these accelerometers because it has hardware specifically dedicated to demodulating the signal and the FCB is more than fast enough to sample all three axes at 50 Hz each. Once again there are a limited number of channels available for PWD, so the three axes share an interrupt pin with two GPIO pins (GPIO5 and GPIO6) controlling a multiplexer. This means that if the two pins get 00 the x-axis is sampled, if they get 01 the y-axis is sampled, if they get 10 the z-axis is sampled, and if they get 11, no axis is sampled and a ground state is output.

Acceleration sensors are currently the BMOO unit's most prolific source of data since their signals are sampled at a much faster rate than the signals from the other sensors. During each round of sampling, a one-byte label and four-byte timestamp are affixed to two bytes of data from each dimensional axis, resulting in eleven bytes per sample. At 50 Hz (50 samples per second) the data generation rate of the accelerometers in this system is 550 bytes per second. The sampling of other sensors currently connected to the BMOO unit occurs twice per minute or less, but attempting to monitor every instance of motion requires numerous acceleration samples to be taken per second. The accelerometers are mounted on a bovine's head since head motion is clearly associated with common activities such as eating and drinking. A special cable has been fashioned which connects to an RJ-45 plug on the BMOO unit and protrudes from a film canister. The film canister is used as an easy means to shield the accelerometers from dirt and water and is filled with protective foam which holds the accelerometers in place and provides additional protection from the environment. This cable uses two wires to provide a power and ground connection from the BMOO unit and uses an additional three wires to relay the three axes of accelerometer data to the TERN FCB.

C.3 Temperature and Humidity

Ambient temperature and humidity can have a clear effect on the core body temperature of warm blooded animals. Extreme temperature variations can have a perceptible effect

on the physical activity level of an otherwise healthy animal. Since cattle can become less active in times of excessive heat or cold, the ambient temperature and humidity can also play a role in determining healthy activity levels as measured by the accelerometers.

The BMOO unit employs a Sensirion SHT11 humidity and temperature sensor [21] and takes a sample every 30 seconds. The validity of the data from the SHT11 is ensured by a CRC-8 checksum that is automatically transmitted alongside the data. The temperature component of the SHT11 can output either 12 or 14 bits of data, where the additional bits provide a better resolution but take longer to acquire. The BMOO unit utilizes the 14-bit option, which provides an accuracy of ±0.4°C, operates in a temperature range from 40°C (-40°F) to 123.8°C (254.9°F), and provides a 0.01°C resolution. The humidity component can be set to output either 8 bits or 12 bits, where resolution is once again improved with a larger number of bits. Using 12 bits, the BMOO unit provides a humidity accuracy of ±3% relative humidity within a humidity range from 0% to 100% relative humidity and provides a 0.05% resolution. This sensor is housed in the same canister as the accelerometers and uses the two remaining wires of the RJ-45 cable to form a Serial Peripheral Interface (SPI) connection between the sensor and the FCB. One of the wires is used as a serial clock input to the SHT11 to synchronize timing with the FCB, and the other wire is the tri-state data line that acts as both the input and output of the SHT11.

Unlike accelerometer and GPS data, data from the SHT11 are not sent automatically at predetermined intervals, so the FCB must act as a controller by initiating data acquisition. This is a fairly simple process because the SHT11 operates with a few basic 8-bit commands. For temperature, the bit sequence 00000011 is sent from the FCB to the SHT11, and following a 300 ms measurement delay, three bytes are transmitted to the FCB. Two of the bytes are measurement data, where the first two bits received are ignored since the result is only 14 bits, and the third byte received is the 8 bit CRC checksum. Humidity is measured and returned similarly except the command bit sequence is 00000101 and the first four bits are ignored since humidity is a 12-bit value. The FCB has a couple of other functions as the controller because the SHT11 sends a

byte at a time. The FCB is responsible for acknowledging each transmitted byte by clearing the data line to a low state and waiting for the next byte to be sent. When all three bytes are received, the FCB must perform error checking using the CRC byte, then set the data line high to signal a successful reception.

The raw data provided by the SHT11 are not presented directly in degrees or percent of relative humidity, so conversion formulas are applied before the data are logged. The formula for temperature is $T = d1+d2*SO_{T,}$ while the formula for humidity is $H = c1+c2*SO_{RH} + c3*SO_{RH}^2$. For temperature, SO_T is the value provided by the SHT11 and is a constant whose value is determined by the supply voltage and desired output units, so at 5 V d1 equals -40.00 for both °C and °F. The value of the second constant, d2 depends on the sample size and the desired output units, so at 14 bits equals 0.01 for °C or 0.018 for °F. For humidity, SO_{RH} is the value provided by the SHT11 and the three constants, c1, c2, and c3, depend on the data size, which at 12 bits are -4, 0.405, and $-2.8*10^{-6}$, respectively.

C.4 HQI Data Reader (Core Body Temperature and Heart Rate)

Development of a custom ingestible bolus to perceive heart rate and core body temperature is underway [22], but the BMOO unit already supports some commercial tools to accomplish the task. In near term, this serves as a method to measure core body temperature and heart rate until bolus development is finalized. As bolus development progresses, this will provide a verified and redundant set of measurements against which to compare data from these newer sensors. One pair of devices that measure core temperature and heart rate are made to interface with either a data logger unit manufactured by HQI Inc or a third party data reader device (for instance a data reader watch developed by Polar) [23] that is able to buffer both sets of data and relay them to the BMOO unit through an RS-232 serial connection.

Core body temperature is transferred to the HQI data reader from a CorTemp ingestible pill manufactured by HQI Inc [7]. The CorTemp temperature measurement electronics are encased in a cylindrical protective layer of epoxy resin and silicone that is four inches

long and an inch in diameter. It is designed to be swallowed by a bovine and weighted such that it remains in the bottom of the animal's reticulum; it does not pass through the digestive system, and it remains in the reticulum during rumination.

The CorTemp pill can communicate its measurements to a wrist watch data reader unit with limited storage capacity or a data logger unit that retains a greater amount of data. The watch is good for immediately viewing measurement results, but it is not integrated into the BMOO unit. The HQI data logger is a standalone unit with a user interface and a menu structure operated by a 16-button keypad and a two-line, 32-character liquid crystal display. It can store up to 110 hours of continuous data at a sample interval of ten seconds and has a battery life of approximately two weeks using a standard 9 V alkaline battery. To supplement the standalone mode, HQI offers CorTrack software that communicates with the data logger via a serial connection. In addition to being able to quickly and easily configure the data logger, the software can pull the data off of the logger, save it to a PC, and visually plot the data. Although the data logger uses standard RS-232 communication, it has a proprietary six-pin MF6 connector. The other end of the manufacturer-provided cable has a standard nine-pin DB9 connector to connect to the serial port of a PC. The BMOO unit uses an RJ-45 connector to interface with the HQI data logger. The data logger's provision to communicate with a PC over a serial line is exploited by the BMOO device in order to integrate heart rate and core body temperature with the other sensor data. Using a two-position switch, a line to the FCB is shared by the BMOO configuration port and the HQI data logger. This line goes through a MAX3233 [24] level converter to get it from RS-232 (0 to 5 V) levels to UART levels (0 to 3.3 V). The HQI data logger, when operated in its PC link mode, can stream data over the serial line, where the FCB collects and stores these data on it own CF card.

Heart rate is transferred to the HQI data reader from a belt manufactured by Polar [23]. The Polar belt design was originally intended for use on horses, but it can suitably sense the heart rate of a bovine with the addition of longer straps to accommodate the extra girth. The belt uses a pair of electrodes (aided by electrode gel to make proper ionic

contact) to acquire heart rate. Placement of the belt is not a significant factor, so long as the belt is securely attached and the gel is placed on the electrodes.

C.5 Digital Angel

A secondary body temperature sensor has been tested with the BMOO unit in the form of the Digital Angel BioThermal System [25]. This is a system with an implantable RFID chip designed to monitor the body temperature of livestock and assign a unique identification number to each individual animal. It was originally chosen because the implant was potentially easy to use, a passive device requiring no power source, and the first implantable RFID chip approved for livestock use by the United States Department of Agriculture as part of the NAIS [26]. Similar to the HQI data logger, the Digital Angel BioThermal System requires a data reader unit to interact with the BMOO unit. The current version of the BMOO unit no longer directly supports Digital Angel although the infrastructure remains to support it in future versions. This decision was made because the Digital Angel system is directional and has poor transmission range. Additionally, subdermal temperature is not synonymous with core body temperature, so clinical usefulness is unclear.

D. ZigBee Implementation

ZigBee is wireless communication specification maintained by the ZigBee Alliance. It is designed for low-cost, low-power radio frequency (RF) networking applications. The ZigBee system used with BMOO is equipped with a Chipcon CC2420 RF transceiver [27] that operates in the 2.4 GHz radio band. The ZigBee communication facet of the BMOO unit utilizes a PIC18F2620 microcontroller and is derived from the design of the Microchip PICDEM-Z ZigBee Demo Kit. The ZigBee Alliance defines ZigBee compliance standards, but the actual implementation is provided by the ZigBee product vender in the form of a software stack. Since the ZigBee portion of the BMOO system is derived from the PICDEM-Z Demo Kit, the initial stack was developed by Microchip, although other compatible implementations exist as noted in section D.1-2.

D.1 ZigBee Stack

The ZigBee Alliance definition of the ZigBee stack architecture [8] is a layered network communication protocol loosely based on the Open Systems Interconnection (OSI) Basic Reference Model [27]. In this model, layers are said to be stacked vertically since each layer only interacts with the layer above it and the layer below it. Typically, communication begins when the layer directly accessed by a programmer, the highest layer, issues a request to a layer below it. This top layer is oblivious to the process involved in fulfilling the request and only knows how to manage the request's completion. The next-lower layer will perform a function or a small subset of functions defined by its role in the model, issuing requests to the layer below it to complete the request. This process continues until the bottom layer is reached and all portions of the request are fulfilled at which point the lower layers can begin the process of notifying the respective upper layers.

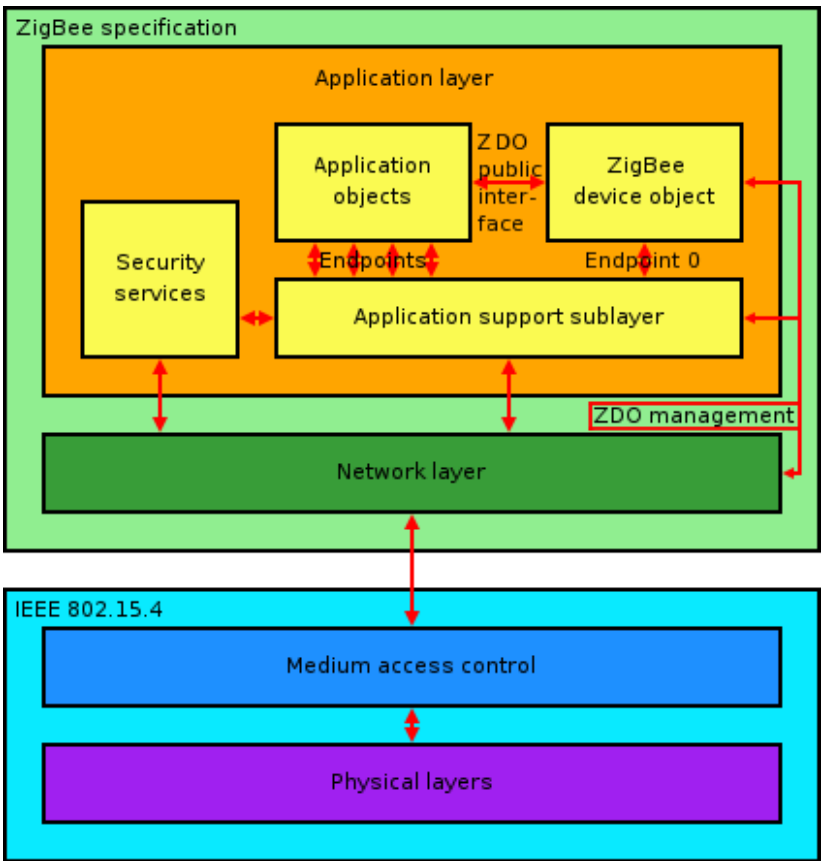

Figure 2. ZigBee Stack Specification

The ZigBee stack, illustrated in Figure 2, defines the following layers: the application layer (APL, the highest layer), the Application Support (APS) sub-layer, the Network (NWK) layer, the Medium Access Control (MAC) layer, and the Physical (PHY) layer. The APL layer contains user applications and is the primary user interface layer; it is aided by the APS sub-layer which provides the connection to the NWK layer. The APL sub-layer also holds ZigBee Device Objects (ZDOs), manufacturer-defined application objects responsible for defining the role of individual devices within the network. In addition, implementation of security features falls under the domain of the APL layer. The NWK layer should not be used directly by programmers; it is responsible for maintaining network connections and routing data, so many functions of the APL rely directly upon it. The MAC and PHY layers are implemented in ZigBee as defined by the IEEE 802.15.4 standard for wireless communications [28]. This means that the MAC layer takes a data stream and organizes it into packets to transmit. During data reception, this layer is responsible for communicating with the lowest layer and performing basic error checking before acknowledging that a packet has been successfully received. The lowest layer, the PHY layer, must use the available electronic components and physically transmit bits from one point to another. This layer is effectively responsible for properly utilizing the RF transceiver to transmit and receive radio signals.

The ZigBee protocol defines a node as any physical device with a single radio transceiver. Node devices are each given one of four possible roles (ZigBee coordinator, ZigBee Router, ZigBee End Device, or Zigbee Device Object) defined in the ZDO layer, and these roles determine their capabilities within the network. Each node then implements stack software that is typically provided by the device manufacturer, although some third party stacks do exist that are compatible with the CC2420 radio transceiver.

D.1-1 Microchip Stack

The manner in which BMOO utilizes ZigBee is based on the Microchip PICDEM-Z demo kit [13], since initial network testing was accomplished with a demo kit and its stack as provided by Microchip. When work began on the BMOO project, the most

recent version of the Microchip stack was V1.0-3.4 [29]. This was not a certified ZigBee-compliant stack, and certification was not granted to Microchip until the recently released V2.0-2.6 [30] - this requires an upgraded radio transceiver to function. The stack we had at our disposal for much of the BMOO development was not certified because it did not support security features (authentication, encryption, access control lists, etc) defined in the ZigBee specification. Second, it only provided support for star network topologies, whereas ZigBee specifies star, mesh, cluster-tree, and peer-to-peer topologies. Star topologies are often used in home/office computer networks, where many PCs connect to a central router. In a ZigBee network, end device nodes are used in the place of PCs and the central router is replaced by a coordinator node. Finally, Microchip's stack only supported two basic device primitives defined by IEEE 802.15.4 (full function devices (FFDs) and reduced function devices (RFDs)), instead of the four defined in the ZigBee specification.

FFDs are programmed with a relatively large set of services and consume a large portion of the microcontroller memory. An FFD is essentially the Microchip implementation equivalent of a ZigBee coordinator, which is the most capable device type in a ZigBee network. Each network must have one and only one coordinator that is responsible for establishing the network, discovering new nodes and adding them to the network, maintaining a neighbor table and binding table, relaying data from source to destination, and enforcing security. The Microchip FFD performs all of these functions with the exception of security.

RFDs, on the other hand, contain a minimal subset of the ZigBee services and are only able to communicate directly with the network's FFD. An RFD is Microchip's equivalent of a ZigBee end device, which is defined by the ZigBee Alliance as a device with only enough functionality to communicate to its parent node. ZigBee end devices typically exist to either be controlled in some way or collect data and relay the information to a parent. For instance, in a network with a coordinator and two end devices, one containing a light and the other a switch, the switch information could be

relayed to the coordinator, which would use the information to send control signals to manage the light.

The neighbor table is an array stored in the nonvolatile memory block of a coordinator and specifies all nodes that have been discovered. Even if a node becomes disconnected from the network, such as by wandering outside of radio range or suffering power failure, the coordinator maintains the node's information in its neighbor table. This allows the wandering node to be reconnected much faster and, more importantly, allows the binding information to remain. Binding information entries for each node in the network are maintained in the coordinator's binding table. This is the ZigBee mechanism that allows a coordinator to accurately route information between independent, disengaged nodes.

Binding is the Zigbee specification methodology for logically linking device inputs to device outputs. While a node is defined as having exactly one RF transceiver, it can have multiple components, and each one is assigned a logical endpoint. For example, if the end devices in the earlier three-node network each had two switches and two lights, the switches would be assigned input endpoints while the lights would have output endpoints. During initialization, each node could then issue binding requests to the coordinator to logically connect each switch to the light on the other device. The coordinator would record this information in the binding table, so that whenever a switch was pressed, its end device would send a message to the coordinator which would dispatch the message to the appropriate end device and toggle the light. This binding cannot only be performed for simple components such as switches and lights, but also for the transmit (Tx) and receive (Rx) lines of the radio transceiver to allow streams of data to be routed throughout the network. Binding can be either direct or indirect. Direct binding is when a binding is made between endpoints on devices that are in direct communication. In a star network this would occur only between an end device and the coordinator. Indirect binding occurs between endpoints on end devices that do not communicate directly with each other, so the multiple switches and lights example is an example of indirect binding.

While the limitations of the Microchip stack prevented it from being ZigBee compliant, none of the omitted features were urgent for BMOO's implementation. The stack does implement all of the defined layers, with the functionality of each layer contained in separate C source code and header files, so network initialization and packet routing is workable. While the ZDO only has two configurations, determined by preprocessor directives, each individual BMOO unit can be configured as an RFD that routes its sensor data to a centralized base station connected to a PC and configured as an FFD. While a mesh topology would help to increase the distance the RFDs could roam from the FFD, the star topology is adequate in allowing sensor data from an RFD to be routed to a central FFD. The stack has a well organized APL layer that supports serial communication, so user applications have been developed that allow the BMOO unit's PIC to get sensor data from the FCB. The APS then allows sensor data to get from the PIC to the central FFD by making calls that rely on the underlying layers.

Although the Microchip stack's limitations did not prevent it from satisfying BMOO's functional requirements, there were some problems with this version of the stack that made an alternative stack desirable. The primary problem is that an RFD (ie a BMOO unit) would often lose communication with the FFD (ie BMOO base station) and would require a hard reset to resume functionality. This problem was so frequent that connections often lasted less than a few minutes before failure. While connections would occasionally last an hour or more, there was never twelve hours of uninterrupted connectivity. The connection time was sporadic, so it was impossible to determine how long a node could stay connected to the network without being reset. This irregular connection issue was unacceptable for sensor networks designed to continuously function autonomously. Some possible explanations for this problem involve a malfunctioning watchdog timer or improper implementation of the RF transceiver, but Microchip never completely fixed the stack problems. The problem was most likely deeply embedded in the design, which could be the reason Microchip completely rewrote the stack and went to a different transceiver in later revisions of the PICDEM-Z kit [13].

D.1-2 Mississippi State Personal Area Network (MSState PAN) Stack

Due to problems in the ZigBee stack provided by Microchip, an alternative stack was required. A license-free stack, the MSState PAN Stack [31], developed by Dr. Robert Reese of Mississippi State University, was discovered. The stack was developed to be highly portable and platform independent, so it is not as hardware restricted as the Microchip stack, which is only licensed for use with a limited number of PIC microcontrollers. However, the MSState stack is also not a ZigBee-compliant stack and implements an even smaller subset of the ZigBee protocol than the Microchip stack, but it has much better network stability. Some of the omitted features include only allowing a single message type, the generic MSG message format. Other ZigBee stack implementations support a key value pair (KVP) message format which is useful for indirect communication between two RFDs. The KVP format allows the FFD to maintain a key/value database, where keys represent variables either on the FFD or on other devices. This lets devices access or change the value of variables that exist on other devices. While this is a useful feature designated by the original ZigBee specification, it is unnecessary for the BMOO application because RFDs do not need to share information with each other: all of the sensor information is destined for the FFD to be uploaded to a computer. Another omitted feature of the MS State stack is that it does not support dynamic binding, so all binding must be application defined and determinable at compile time. Dynamic binding is a feature more associated with mesh networks or in applications where RFDs need to be in indirect contact. Once again neither of these cases is required for BMOO since RFDs only transmit their data sets to an FFD. While this stack may not be completely ideal for achieving ZigBee compliance, its workability and intuitive, flexible design have made it the best option for implementation in the current BMOO prototype.

E. BMOO Network

Although most testing to date has been done with single animals, the BMOO network is designed to consist of the numerous BMOO units, each mounted on an individual animal. These BMOO units communicate with a single ZigBee base station responsible for transferring all data to a PC base station. The PC base station will then enter the data into an application specific SQL database, where they can be permanently stored for future analyses. This opens the possibility of entering the data online, where near-real-time herd information can ideally be made accessible.

E.1 BMOO Units

The network functionality of a BMOO unit is currently driven by a PIC18F2620 (PIC) microcontroller [12] employing the MS State PAN ZigBee implementation. This microcontroller only has 2 MB of memory to store both programming instructions and data variables. As such, it is incapable of collecting a large amount of data, and acts as an intermediary between CF temporary storage and permanent storage on a PC for one data packet at a time. This communication is made possible through a UART connection to the FCB to transmit data and a link line connection to signal the FCB when the PIC is ready to process data. The link line is a simple connection of general I/O pins between the PIC and the FCB that are set when a ZigBee network is established. Since networking is the PIC's only function, it initiates data transmission, so the link line is an output at the PIC and an input at the FCB. During the main loop of the FCB (while sensors are being polled), the FCB also checks the link line to see if it needs to send data to the PIC. Data transfer is the first priority, so if the PIC sets the link connection, the FCB will retrieve a single packet from the CF card as soon as it has finished its current sensor acquisition.

BMOO stores data on the CF card in a rather primitive fashion: a single file is created to hold data from all of the sensors in 512-byte sectors. Before data are recorded onto the CF, each sector is prefixed with a unique character tag ('G' for GPS, 'A' for acceleration, 'E' for environmental, 'C' for core temperature and heart rate, 'D' for

Digital Angel, and ‘L’ for TERN log messages) and the time the sample was taken. The character tag is useful for decoding the data file system because once the tag is identified, the amount of data until the next identifying tag is known, effectively making it a delimiting mechanism.

When the PIC indicates that it is ready to process data, the FCB grabs a sector of data from the CF card and encapsulates it into a BMOO packet. Each BMOO packet is 521 bytes and consists of four different fields. The first four bytes contain a device number that is unique for each BMOO unit in order to identify the data’s source animal. The next four bytes contain a packet number as a means of sequential data transmission/reception to detect dropped packets and ensure data integrity. The next 512 bytes are the payload data, which are a copy of the current sector of CF data. Finally, a one-byte CRC-8 checksum is calculated and attached to the end of the BMOO packets as yet another means of ensuring data integrity.

After a packet is formed, it advances from the FCB to the PIC for its first step through the network. Once the entire packet is sent through the UART line, the PIC begins to process and transmit it while the FCB waits for a reply. The FCB does not try to send any additional data to the PIC or move on to a new data sector until it receives a successful acknowledgement. Since the transmission is done using ZigBee, the BMOO packet must be broken up and encapsulated into multiple ZigBee packets. The encapsulation process is handled by lower layers in the ZigBee stack, so only application-layer messages are needed to send data from the BMOO unit to the BMOO base station. Since this ZigBee implementation relies on a 2.4 GHz radio transceiver, much can go wrong during data transmission. This is amplified by the fact that 2.4 GHz can be prone to collisions since it is a public band used by an increasing variety of devices such as cordless phones and wireless Ethernet routers. By design, the lower layers of the ZigBee stack provide mechanisms to ensure proper transmission and avoid collisions, but a number of retransmissions may be required before each packet reaches its destination. While the MSState stack is capable of sending 512-byte packets, the unpredictable nature of radio transmissions makes it desirable to send much smaller packets in an effort to

minimize retransmissions and packet loss. However, creating packets that are too small adds too much processing and networking overhead since more packets must be encapsulated. As a compromise between reliability and processing requirements, the PIC breaks up each BMOO packet into ten packets; nine 55 byte packets and a final 26 byte packet.

As soon as a complete BMOO packet is sent from the PIC to a base station, it waits for a positive acknowledgment from the base station. The next section covers this mechanism in more detail, but once a complete BMOO packet has been received and the CRC has been verified, the base station sends a positive acknowledgement in the form of a three-byte message containing the string "ACK." Conversely, if something goes wrong and the CRC does not check out, a negative acknowledgment is sent from the base station to the PIC with another three-byte message containing the string "NAK." Whatever the result, the PIC immediately relays the acknowledgment string to the FCB. As the FCB waits, it continues to monitor the UART buffer for the acknowledgment string. If a positive acknowledgment is received, the FCB will invalidate the transmitted sector, prepare the next sector, and return to the main loop. If, alternatively, a negative acknowledgment is received, the FCB doesn't invalidate or alter anything, but rather returns to its main loop. This entire process is repeated until no new data exist on the CF card in which case the link line is ignored until data become available.

E.2 Base Station

A BMOO network contains a single comprehensive base station device that consists of a microcontroller device connected to a PC base station. Currently, the microcontroller is a Microchip PICDEM-Z demo kit which includes a PIC18F4620 [12] driven by an external crystal oscillator, a serial port, level converters, and a Chipcon CC2420 RF transceiver [27]. Using the serial port, a base station can stream data to a PC either running an SQL database or making entries into a remote SQL database.

The base station is the central node in a BMOO network where all sensor data are eventually sent for permanent storage. The flow of data is made possible by a series of state machines running on each of the ZigBee-enabled microcontrollers. This processing begins when a BMOO unit signals the BMOO base station that a packet is ready to send. The base station's state machine then goes into a data reception state where it receives Zigbee packets. Once ten packets have been received, a reconstruction state is entered and the base station recapitulates the multiple packets into a single BMOO packet. At this point, the base station calculates the CRC to verify data integrity, but it only replies to the BMOO unit if the checksum is invalid. If the checksum passes, the base station enters a serial communication state, where it uploads the BMOO packet to the PC. The PC receives these packets and begins the process of permanent storage. First, the PC performs the final CRC calculation and verifies sequential transmission by checking the packet sequence number with the previous packet. Next, it extracts the device number and the payload data from the BMOO packet. It then grabs the first data-type tag it finds in the payload and uses it to determine how to properly extract the individual data fields. Once all data fields are known, the tag and device number are used to insert the data into the proper SQL table. This continues until a BMOO packet is entirely processed or the remaining data are smaller than the tag indicates, in which case it is buffered until the next packet is received.

When all data are successfully entered into the table, the PC sends a three-character "ACK" packet to the BMOO base station, which relays the message to the source BMOO unit. However, if at any point in the process a CRC check is not passed, the base station discards current data, sends a "NAK" packet and goes to a wait state. This procedure leads to relatively long times between packet transmissions because a new BMOO packet cannot begin to be processed by the FCB until it has been completely sent to the BMOO unit PIC and verified, sent to the BMOO base station and verified, sent to the PC, verified, and entered into the database. While this is time consuming, it minimizes packet loss and ensures that no data are discarded from temporary CF storage until they have been deposited in permanent storage.

F. Future Work

While a great deal of development time has been spent on the current prototype BMOO unit and base station, the technology supporting it is quickly becoming outdated. For instance, Compact Flash technology (once considered a miniature storage solution) has been replaced by smaller, faster solid state technologies such as MicroSD, MMC, or even Smart Media. While the TERN microcontroller system is a robust platform, it is too bulky and cumbersome when compared to recently released devices of a similar nature.

One possible solution exists in the form of mote modules such as the MICA2 developed by Crossbow [32]. A mote is a small, scalable, low power module for use in a wireless sensor network. As such, a number of different sensors could be placed on a single mote which would have the ability to talk to another mote acting as a base station. Motes can be made to house all of the different external sensors currently operating with each BMOO unit. There would still, however, need to be work done to develop a sensor pill capable of communicating with a mote, but since motes also support UART and serial connection this could be accomplished. While the sensor development would be significantly different than with the BMOO unit, much of the behavior could be ported over from a BMOO unit to a mote. The MICA2 also relies on ZigBee technology for wireless network communication but implements more features than either the Microchip stack or the MSState PAN stack, making it a truly ZigBee-compliant device. The combination of these factors would make a mote-based system ideal for future revisions of the BMOO unit and base station.

Finally, with a flow of sensor data established, more work can focus on the back end of the network after the data have been stored on a PC. Initially, this could include improvements to the existing SQL database or the proliferation of the database into a larger scale infrastructure, including multiple locations and a central database. This could be further expanded with the creation of a web server to process these data in near real time and provide visual plots and health tracking algorithms. Eventually, this could lead to signaling alerts when an individual animal shows signs of illness, so the animal can be inspected and quarantined in an effort to minimize and track the spread of disease.

CHAPTER 4: INDUCTIVE LINK – MOTIVATION AND THEORY

A. Motivation

Chapter 3 discussed a prototype wearable unit and the assortment of sensors connected to it. To attain a more robust monitoring design for long-term use as well as improve the fidelity of the sensor data, it will be helpful to have internally positioned sensors to capture vital data from within the animal (such as heart rate, core body temperature and respiration rate). Sensor design itself is a nontrivial issue, and most commercially available sensors provide only one metric, as seen in Chapters 2 & 3. A more efficient and compact solution would be to have an extensive lab-on-pill solution capable of measuring an array of commonly accepted health parameters [33] [34].

Work is underway at KSU to develop a solution to this problem by designing a custom pill that measures heart rate, core body temperature and respiration rate in a single package [22]. However, these data will need to be transferred from within the animal to the outside world for analysis. Most wireless communication modalities are designed to operate in the ambient air environment; not through biological tissue. This chapter will discuss a communications link based on the principle of magnetic induction. These types of links have been around for years in a variety applications [33-47], but due to their limited range, their application has not been very widespread. Magnetic induction has been used in human applications for devices such as cardiac pacemakers [48] or gastrointestinal endoscopes [38, 39]. However, these customary approaches become problematic when considering the tissue volume of cattle; an internal sensor may see a distance of separation of up to several feet between itself and an external reading device.

B. Magnetic Induction Versus Radio-Frequency Communication

Magnetic induction communication is related to radio wave communication given that they are both wireless technologies that employ electromagnetic (EM) fields. The two technologies also rely on antennae to transmit and receive signals, although the antenna

design process is fundamentally different. Both technologies rely on the same basic principle of using a transmitter to radiate a signal through space such that the signal can be wirelessly detected by a remote receiver. The most notable difference between the two communication technologies lies in the region of the EM field in which they operate and thus the component of the EM field utilized (i.e. near-field versus far-field).

Magnetic fields and electric fields cannot subsist without one another. Their relationship is similar to that of a voltage potential and a current; whereas a voltage potential is measured in volts and a current is measured in amperes, an electric field is measured in volts per meter and a magnetic field in amperes per meter. Magnetic induction is a phenomenon associated with the magnetic field. Magnetic field strength, H (A/m), relates to the passage of current through an electrical system and tends to be the dominating portion of an EM field in the region close to the transmitting antenna, known as the Fresnel region or simply the near-field region. When you multiply the magnetic field strength by the permeability of the medium, μ (H/m or N/A^2), you get the magnetic flux density, B (T or Wb/m^2 – sometimes known simply as the magnetic induction). As the radial distance from the antenna increases, the magnetic field strength tapers off until it becomes negligible, and the EM field becomes composed almost entirely of the electric field strength, E (V/m), a concept relating to the strength of electric charges rather than their movement. The reasons for these E and H relationships will be further discussed in the theory section of this chapter. The portion of an EM field where E dominates is known as the Fraunhofer region, or simply the far-field region, which is the operating region for radio-frequency (RF) applications.

RF technology is the dominating wireless technology primarily due to its long range capabilities. Another important factor is the relative simplicity of the EM field in the far-field region. In the far-field, the signal is generally unidirectional, planar and defined by a highly structured wave that can be categorized by its amplitude, phase, and frequency. The amplitude of this electromagnetic wave often oscillates in a sinusoidal manner with respect to both space and time. The peak amplitude is a measure of the signal's strength and decreases as the wave travels further from the transmission source. Frequency is a

measure of the speed at which this wave oscillates. Electromagnetic waves at multiple frequencies exist simultaneously in free space with interference occurring only between signals with identical frequencies. As such, the radio frequency spectrum (3kHz – 300GHz) is highly regulated with international standards bodies defining specific ranges of frequencies (bands of the spectrum) and governing acceptable applications for each band through frequency allocation. For example, amateur shortwave radio operators are not allowed to operate on frequencies allocated for AM (535 kHz – 1605 kHz) or FM (88 MHz – 108 MHz) radio broadcasts.

The absorption characteristics of RF signals are their downfall when considering for use with internally placed devices. When a wave is transmitted to a medium, it can be propagated, reflected, refracted, absorbed, or scattered. Radio-frequency waves propagate rectilinearly in free space, but large portions of the energy are absorbed or scattered as they propagate through water or tissue. While these propagation distances depend on frequency ranges, a typical radio wave can penetrate a fraction of a single wavelength through a biological medium before detrimental signal attenuation occurs. While RF technology could be effectively applied to subcutaneous placements (i.e. implants just below the dermis), this technology is unsuitable for transmissions originating from the inside of a large animal.

Magnetic induction, being a near field phenomenon, naturally tends to be a short range technology. Generally, the near field is defined as being within the radius of a single wavelength from a transmission source. The near field of a dipole antenna is therefore considered spherical rather than planar. This signal is also directional since the antennae's pole orientation affects the field strength. The near field is more complex to measure and model than the far field, since the magnetic and electric portions of the signal exhibit a more complicated spatial relationship. The primary cause of this complication relates to the impedance of the wave, Z. The magnitudes of E and H are directly proportional to each other with the relationship $|E| = Z*|H|$. This is another reflection of the analogy of the E and H fields to voltage and current since the derivation of the formula leads to Ohm's law which states $V = I*R$, and in fact Z, like R is measured

in ohms (Ω). The far field maintains relatively simple, constant wave impedance equal to the characteristic impedance of the medium (377Ω for free space). Contrarily, the wave impedance in the near field is affected by the transmission medium as well each pole of the transmitter and complex interactions between the poles and the medium leading to a complex, multidimensional wave impedance.

The far field is usually modeled as being uniform; however, the near field must be modeled with a number of subdivisions, which is further complicated by the fact that these regions don't always have clear boundaries. Instead, boundary transitions often change with time and occur gradually in space, where certain positions may experience a combination of characteristics from multiple regions. First, there is a reactive portion of the near field in which a large amount of energy is stored, but this energy quickly decays with distance at a rate approximately proportional to $1/r^3$, where r is the radial distance from the source [49]. Reactivity generally dominates up to a range of $r = \lambda/2\pi$ but may exist up to the distance of a single wavelength. The radiating portion of the near field is the transition from the near field to the far field. While there is still some available stored magnetic energy that can be utilized, energy generally begins to disperse rather than be stored. In this region, the energy does not fall off quite as fast as it does in the reactive region: it decays at a rate close to $1/r^2$. The characteristics of the radiating near field can become apparent at $r = \lambda/2\pi$ and last until $r = 2D^2/\lambda$, where D corresponds to the length of the antenna [50]. Finally, there is a transition region where the near field characteristics related to the magnetic field and induction gradually decreases to a point where the electric field overwhelmingly dominates in the far field, the wave impedance become equal to the impedance of the medium, and the wave amplitudes decay at a rate proportional to the inverse of the separation distance (i.e 1/r).

Although near field interactions are limited in range and can be more complex to mathematically quantify and predict, technologies that utilize the near field offer distinct advantages over the dominating far field technologies. First and foremost is the fact that near-field technologies rely on quasi-static magnetic fields rather than propagating waves, so penetration through a medium does not have as detrimental of an effect on

signal transmission. Second, near field applications generally consume less power and occupy a smaller physical space since they require fewer and less complex components. This is primarily because most far-field applications are RF designs that occupy an unlicensed frequency band shared by many different devices. As such, processing overhead is required for channel and frequency allocation as well as more complex signal modulation and keying. While inductive links can share a frequency band, slot allocation is not as much of a concern, since the signals are distance limited and interference is therefore much less likely. Additionally, RF link frequencies are much higher than inductive links, so RF signal amplification would need to be done with components that can support a much larger bandwidth and therefore consume more power. Another reason more power is consumed by far field applications is that the typical goal is to propagate a signal over much greater distances; this must be done at the expense of power draw. Finally, security is not as big of a concern for inductive links; since their transmission range is limited interception is much less likely.

C. Magnetic Induction Theory

Magnetic inductive communication (a.k.a. magnetic coupling, inductive coupling or near field communication) is a short-range wireless communications technology that uses induction coils (inductors). Since this technology relies on magnetic and electric fields, its properties are defined by Maxwell's equations, specifically Ampere's law and Faraday's law of induction, although Gauss's law for magnetism applies to a lesser degree [51] [52]. Ampere's law is the most important in designing the magnetic induction transmitter because it describes how a magnetic field is generated around a conductor through which current is passing. Faraday's law, on the other hand, is useful for the receiver design because this law describes how magnetic fields create electric fields which in turn produce voltage potentials.

Magnetic induction communication works in a similar manner to a transformer where energy is passed from a primary coil (transmitter) to a secondary coil (receiver). The primary difference is that in transformers the separation distance is fixed, so the coupling is constant; however, with magnetic inductive communication, this distance frequently

changes, so the coupling factor is variable. Transformers vary in design but often consist of two loops of wire on separate parts of a magnetic core (often iron); however magnetic induction uses two separate loop dipoles, each of which has a own core. As a result, a properly designed transformer has a fixed geometry and orientation. For inductively coupled communication, since the two dipole coils of wire exist as separate entities, the relative position of the positive and negative poles can have a profound effect on the quality of the signal seen at the receiving coil.

C.1 Ampere's Law Applied to Magnetic Inductive Communication

Ampere's law states that a current passing through a conductor will create a magnetic field surrounding the conductor. For a conductor surface S, Ampere's law appears in integral form as $\int_S B \cdot d\ell = u_0 I$, where B is the magnetic flux density, $d\ell$ is the differential length that encloses the surface, u_0 is the permeability of free space given as $4\pi * 10^{-7}$ N/A^2, and I is the current passing through the surface. In the case of a circular loop of wire of radius r, as used with inductive communication, one can find the partial B-field, ΔB, at the center of the coil caused by each segment of wire, $\Delta\ell$. The integration with respect to $d\ell$ with over the surface becomes the area of the coil, $4\pi r^2$. This leads to the equation $\frac{\Delta B}{\Delta \ell} 4\pi r^2 = u_0 I$, which yields $\Delta B = \frac{u_0 I}{4\pi r^2} \Delta \ell$. The total B field can be found by adding the partial field over the entire circumference of the loop, $2\pi r$. This results in a total B-field at the center of a circular loop of conducting wire of $B = \frac{u_0 I 2\pi r}{4\pi r^2} = \frac{u_0 I}{2r}$ [50].

This value can be amplified with additional design elements. For instance, the previous equation applies to a hollow coil of wire, so only the permeability of free space is taken into account. The B field can be improved through the use of a core with larger permeability, u_r. In this case, the resulting permeability becomes a product of the two: $u = u_0 u_r$. Also, a single loop of wire is not typically used to create an inductive antenna,

rather it consists of a coil of wire with multiple turns wrapped around a solenoid core in order to increase the inductance of the antenna and strengthen the field such that $B = \frac{uNI}{2r}$ at the center of the solenoid. Finally, it is not the center of the solenoid that is of interest, but rather a point at radial distance, *x*, away from the solenoid. Putting all of this together, the B field at distance, x, due to a coil of wire with radius, r, and permeability, *u*, is defined as $B = \frac{uNIr^2}{2(r^2 + x^2)^{3/2}}$. In cases where x is much larger than r antenna, this equation can be simplified to $B = \frac{uINr^2}{2x^3}$.

The B-field equation reveals some important information in regards to inductive communication and antenna design. First, the variable that appears to have the most impact on the B field, the separation distance, is related inversely to B. This simply means that as the separation distance increases, the strength of the B field decays at a cubed rate. The second most influential variable is the radius of the antenna, whose square is proportional to the generated B field. This means that smaller antennas naturally perform poorly, so it is desirable to keep the antenna radius as large as possible to best counteract the effect of separation distance. The remaining variables are directly proportional to the B-field strength, so to maximize the B-field amplitude it is ideal to use coils with many windings, a core with a maximum permeability at the frequency of operation, and as much current as is safe through the transmitting coil.

C.2 Faraday's Law Applied to Magnetic Inductive Communication

While Ampere's law describes how a magnetic field is created around a conductor, it is Faraday's law of induction that describes how this can be used to create a voltage across the terminals of a second coil. Faraday's law in integral form is $\int_S E \cdot d\ell = -\frac{\partial \Phi_B}{\partial t}$, where E is the electric field, $d\ell$ is a differential element, and $\frac{\partial \Phi_B}{\partial t}$ is the partial time derivative of the magnetic flux with respect to time. The negative sign in front of the flux derivative

indicates that the electric field created by the flux always reacts in opposition to the magnetic flux. The magnetic flux is a measure of the magnetic induction from a given surface and is defined as $\Phi_B = \int B \cdot dS$. This is an important equation because it demonstrates that the electric field of the receiving coil is dependent on the magnetic flux, which relies on the dot product of the vector quantities of the surface area and magnetic flux density. As a result, coil orientation has a major impact on the induced electric field especially when the coupling factor is small due to a large separation distance between the two coils. This becomes more apparent when the integral is performed based on a round coil of wire, because it results in a flux of $\Phi_B = 4\pi r^2 B \cos\alpha$, where α is the angle between the wire and the point with radial separation, x. It now appears obvious that the flux is at a maximum when α is zero and that the strength decreases if the angle changes, even when the radial distance remains unchanged.

$\int_S E \cdot d\ell$ describes the electromotive force (EMF), $\mathcal{E}$, which in this case is essentially a voltage source created as a result of mutual inductance. Using a solenoid coil of wire as described earlier and applying the equation for magnetic induction leads to an EMF of $\mathcal{E} = -4\pi r^2 N \frac{\partial B}{\partial t}\cos\alpha$. A properly tuned inductive pair will perform substantially better than an untuned pair. This can be seen when the quality factor of the signal, Q, becomes a parameter for the EMF leading to $\mathcal{E} = -4\pi r^2 QN \frac{\partial B}{\partial t}\cos\alpha$. Once again, the negative sign indicates that the EMF is created to oppose the B field. This equation demonstrates that not only is the voltage delivered to the receiver dependant on the antenna radius, orientation and available B field, but it is also directly proportional to the number of turns in the coil and the Q factor created due to resonant tuning.

C.3 Gauss's Law Applied to Magnetic Inductive Communication

Ampere's law and Faraday's law describe the process of creating a magnetic field with a transmitting coil and using that field to induce a voltage on a receiving coil. Gauss's law for magnetism helps to more completely describe the magnetic field. In integral form, Gauss's law for magnetism appears as $\int_S B \cdot dA = 0$ and basically states that the net magnetic flux from a surface is always zero. This is important because it demonstrates that magnetism cannot exist with a single pole but is only possible with dipoles. It also helps to visualize magnetic flux lines from a dipole by demonstrating that the magnetic field is a closed system and that all the energy emitted from one pole must eventually converge at another pole. However, this equation should not be confused with the magnetic flux that appears in the equation for Faraday's law since the flux shown in Faraday's law is obviously not always zero. The Gauss's law equation relates to the net flux created by the transmitting coil, and the flux equation which appears in Faraday's law is a subset of the net flux that intersects with the surface area of the receiving coil.

D. Inductive Antennae Theory

One of the most crucial elements of an inductive link is the antennae. Since it is not viable for an ingestible pill component to be very large, antenna design becomes complicated by the fact that longer transmission distance correlates to increased radius. However, there are still a few variables which can be adjusted to maximize the B-field which include: permeability of core (u_c), number of turns (N), quality factor (Q), and the current through the transmit inductor (I). In addition to increasing the B-field, the variables related to the physical construction of the antennae, u_c and N, increase the inductance value of the antennae, L.

Permeability describes the degree to which a given material reacts to an applied magnetic field. While permeability is dependent on the material, there are a number of factors that can affect its value. These can include signal frequency, temperature, and objects in contact or near the material; the most important of these is the frequency. As a result, when choosing a material to use as an inductive core, it is essential to make sure its

permeability remains high at the frequency of operation. Some of the most common materials commonly operating as inductive cores are ferromagnetic in nature. Ferromagnetic materials come in a wide variety of types from a number of manufacturers and one such manufacturer is the company Fair-Rite Products Corp [53].

The number of turns of the antennae refers to the number of times wire is wrapped around a core. When referring to wrapping wire around a core it is typically understood that this means a complete revolution around the core with no separation between the wire and the core as well as the previous and next full revolution of wire. This is the rule of thumb because any introduction of separation (either between turns or from the distance of the core) leads to deviations from the calculated L value to the actual L value of the constructed inductor. Turns can be wrapped on a single layer or multiple layers of coil. In order to avoid limiting the B-field when implementing a multilayer inductor design, the turns of each layer must all go in the same direction (so each layer must begin at the same point) in order to maintain a single B-field rather than multiple, opposing B-fields that negate each other. Single layer coils have the advantage of being easier to calculate exact value of inductance; however, a large number of turns may require an antenna whose length is not feasible for internal placement. The use of multiple layers can lead to difficulties in estimating the actual value of inductance (or turns needed to create a specific L value) due to interactions between layers and differing radii of each layer due to the thickness of the underlying coils (thickness of the wire multiplied by each layer of winding). However, multiple layers provide an antenna with a fixed length while simultaneously increasing the total radius of the antenna.

The Q-factor is a variable that relates to the signal quality at the antennae operation frequency. This variable comes into play as a result of the antennae being composed of not only an inductor, but also a capacitor. Antennae operate more efficiently when the inductor and capacitor values are tuned to the correct resonant frequency. Resonant frequency is essentially the frequency at which a system (in this case an antenna, although resonance applies to many applications) best oscillates. As a result, when a voltage signal is applied to an antenna at resonance, the largest possible voltage is

induced across then antenna, thus leading to the largest possible radiated B-field (conversely, a wireless signal at the resonant frequency of an antenna is more efficiently perceived). The principle works very much like a singer who can break a glass simply using their voice. While singing loudly helps, it is not necessarily the volume that causes the glass to shatter, but the frequency of the note sung. This is because the glass will tend to vibrated better at its resonant frequency and if done correctly, this vibration becomes efficient enough to compromise the structure of the glass and cause it to shatter. Resonant frequency, $f_{0,}$ is key component of antennae communication and for maximum efficiency, a transmit antenna and a receive antenna must both be properly tuned to this frequency which is defined mathematically as $f_0 = \frac{1}{2\pi\sqrt{LC}}$. This equation shows that resonance becomes constant for fixed values of inductance and capacitance, so resonance can only be manipulated by changing one of these values in an antenna. This formula holds true whether the inductor and capacitor are in parallel or series arrangement and, depending on the application, the L or C components can be made from variable components (such as trimpots or trimcaps).

Typically in inductive communications, a custom made, fixed value inductor is used alongside a variable tuning capacitor (trimcap), so that the capacitor can be adjusted to achieve a maximum Q. Inductive communications consists of at least two antennae, one to transmit and one to receive, but since the resonant value is independent of the L/C arrangement, different arrangements are used for different antennae functions. Since the purpose of the transmit antenna is to create as large of a radiating B-field as possible, the inductor and capacitor are best arranged as a series pair, such that the current through the inductor is maximized. The receiving antenna, on the other hand, seeks to convert as much of the B-field as possible to a voltage drop, as such, the inductor and capacitor are best arranged in parallel, so no unintentional voltage division occurs. While it is the circuitry connected to the antennae that control the input current to the transmit inductor and the detection of signals across the receiving inductor, the proper L/C configuration can ensure that the B-field and detection range is maximized for a given signal.

Finally, the induction value, L, is largely responsible for the creation of the B-field and this value is determined by the physical make up of the antennae. Generalized formulas define the L value of a cylindrical coil of wire as $L = \frac{KuN^2A}{l}$, where A is the cross-sectional area of the coil (in m^2), l is the length of the coil (in m), and K is the inductance modifier also known as the Nagaoka coefficient. The inductance modifier is simply a variable that accounts for the difference between the length of the winding and the length of the core, such that K = 1 when the two lengths are identical. However, when using ferrite cores, the core's manufacturer may provide a more precise modified version of the formula specific to the core material. In the case of the core used for this application (Fair-Rite Antenna RFID Rod 3078990911), Fair-Rite uses the same general formula.

CHAPTER 5: INDUCTIVE LINK – BACKGROUND AND DESIGN

A. Overview and Background

This chapter details a few design iterations of a coherent magnetic induction wireless communication link developed for this cattle monitoring effort. The chapter starts with the original proof-of-concept design used to determine if this type of link would be feasible for use with an ingestible pill. The two goals of these early studies were (1) to determine the effects of submersion in a biological medium on the transmitted signal characteristics and (2) to assess whether appreciable wireless transmission distances could be achieved with this technology. When the proof of concept unit yielded promising results, the design was used as a reference to create two designs operating at different frequencies. The first design operated in the high frequency radio band at 3 MHz: the low end of the frequency spectrum for short-wave radio. The second design operated in the low frequency radio band at 125 kHz: a band allotted to ham radio.

The use of the 125 kHz transmission frequency is noteworthy because it is a standard operating frequency for low frequency radio-frequency identification (LF RFID) systems [54]. LF RFID is an emerging technique to track and distinguish products, people, and livestock. Traditional LF RFID applications include wireless asset tracking (e.g., as a supplement to bar code systems) and security (e.g., digital keys for building/room access or computer authentication), but in recent years the technology has gained popularity as a means to track livestock (e.g., subdermal implants) and manage hospital patients (e.g., RFID wristbands). While LF RFID has proven successful for these earlier applications, none of these products are designed for deep internal placement or to deliver large data payloads. Instead, they typically rely on an externally placed or moderately subsurface transponder broadcasting to an RFID reader, where the payload may be a 12-byte unique identification number accompanied by a few control bits [55].

While LF RFID systems can help to provide a conceptual foundation for the design of this inductive link, including a basic architectural model and set of supporting standards,

a 3 MHz design was also implemented with the thought that its higher carrier frequency may lead to a greater modulated data rate but still allow transmission through tissue. This was driven by the desire to obtain a real-time operational mode, where all physiological data were transmitted from inside an animal. In that context, the communication link cannot become a bottleneck for the transmission of data collected by the ingestible pill. The remainder of this chapter will discuss the design of the various components of these prototypes, including their antenna, transmitter, and receiver designs.

B. Proof-of-Concept Prototype Design

Inductive communication technology appears to be compatible with ingestible devices used for cattle health monitoring, but before significant time and resources were invested in the idea, an initial proof-of-concept design was developed by Patrick York to assess whether a non-air transmission medium would cause detrimental signal attenuation. The design was modeled after a design detailed in a Microchip technical manual [9].

B.1 Antenna Design

A rudimentary approach was taken to the initial design of the proof-of-concept inductive antennae. Plastic-insulated wires were wrapped around empty paper towel rolls, creating air core antennae. While this design was not ideal for implantation, it allowed the team to assess signal transmission through a (simulated) biological medium versus free space.

B.2 Transmitter Design

The basic transmitter design operated on a 3 V power source and was a simplified version of an inductive communication link detailed in a Microchip application note [9]. It called for a 375 kHz square wave to be created by exploiting the dual threshold hysteresis action of a (SN74LS132) Schmidt trigger NAND gate [56]. This square wave was then inverted and combined with the original signal to create a modulated data signal – a 20 kHz square wave for testing purposes. Modulation was accomplished by using a NAND gate to combine the data signal and the carrier. Two separate modulated signals were created (one for the original carrier and one for the inverted carrier), with one going into one input of a half-bridge transistor circuit and the other going into the second input of the half-bridge, in order to double the output voltage of the signal before reaching the final

load of the transmitting antenna. The transmitting antenna consisted of an inductor connected to the output of the half-bridge transistor circuit, and a capacitor connected to ground. Figure 3 shows the transmitter schematic (Eagle Spice; Patrick York).

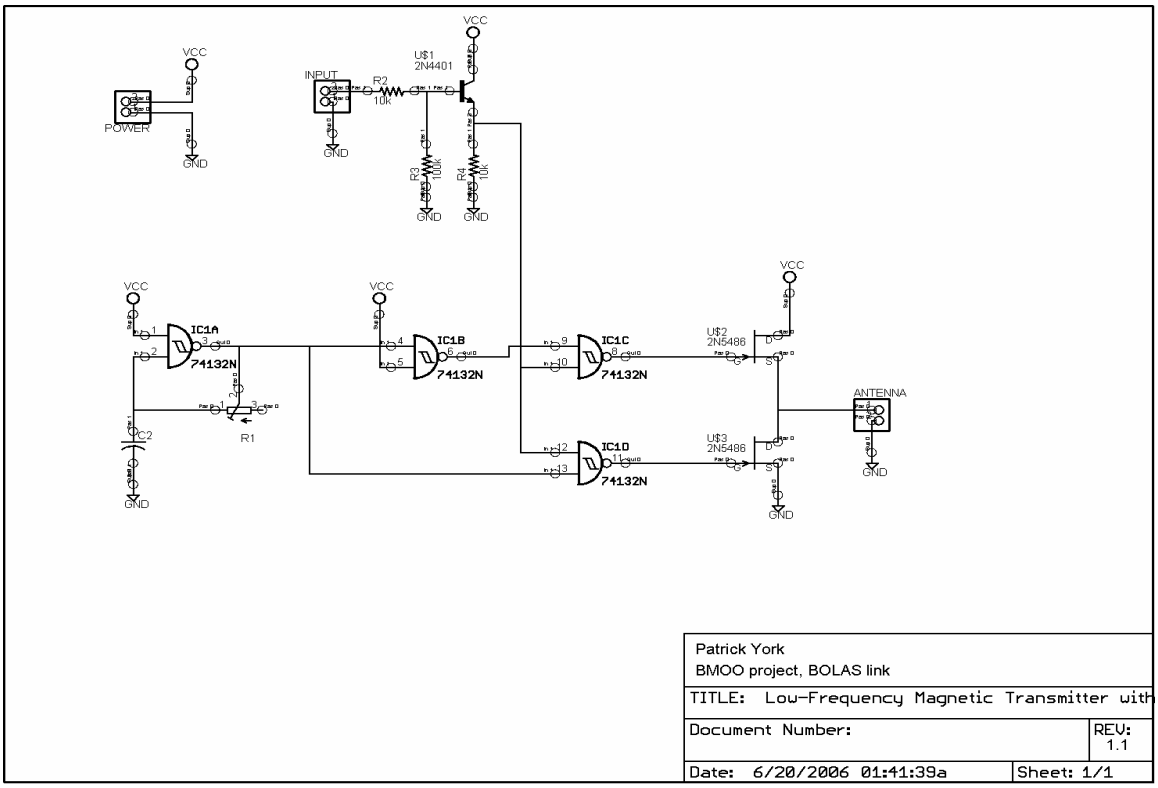

Figure 3. Original prototype transmitter schematic.

B.3 Receiver Design

The proof-of-concept receiver design was more complex than the transmitter and deviated significantly from the original Microchip design. The Microchip design was made with PIC microcontrollers, whereas the BMOO design was entirely analog circuitry. The BMOO design received the signal from the antenna, buffered it, and amplified the signal with a cascaded transistor amplifier. Once the signal was amplified, a half-wave rectifier was used in unison with an envelope detector to extrapolate the data signal (20 kHz square wave) and discard the carrier. Finally, a voltage comparator was used to clean up the signal and scale it to proper voltage levels. Figure 4 shows the receiver schematic (Eagle Spice; Patrick York).

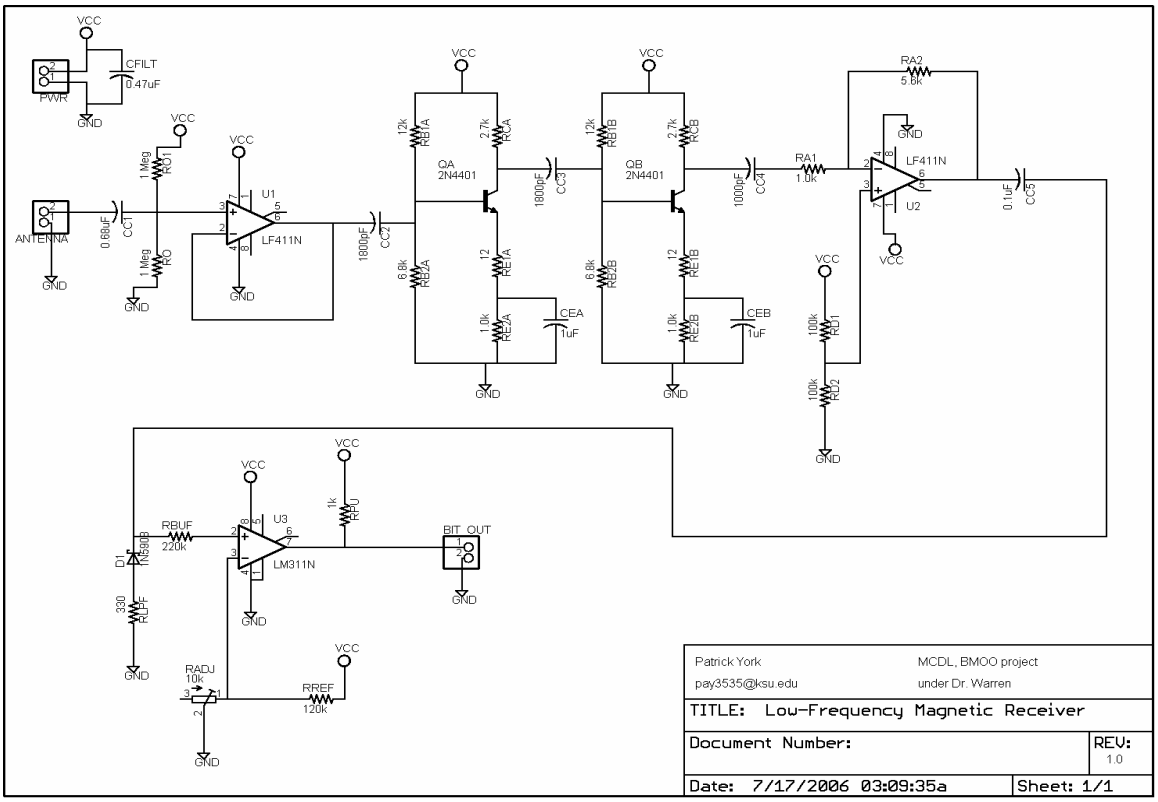

Figure 4. Original prototype receiver design.

C. 3 MHz Prototype Design

Once the original concept was perceived as feasible, a second prototype was designed to address flaws in the original design and to increase transmission data rates. The operating carrier frequency was changed to 3 MHz. This carrier could allow data transmission speeds an order of magnitude greater than previous designs, helping to prevent this link from becoming a bottleneck for the overall system (although for comparison purposes, the data rate was kept at 20 kHz during testing). While this change alone would imply the need to redesign the antennae, they were in urgent need of a redesign in order to reduce their dimensions (by incorporating ferromagnetic cores) and to increase the coupling factor of the pair (by better tuning the resonant frequency of each antenna). Next, the transmitter design was adjusted to increase the strength of the magnetic field around its antenna. Finally, the receiver was completely redesigned to accommodate the change in operational frequency, increase gain, and change the demodulation technique. Figure 5 shows the schematic for the entire system.

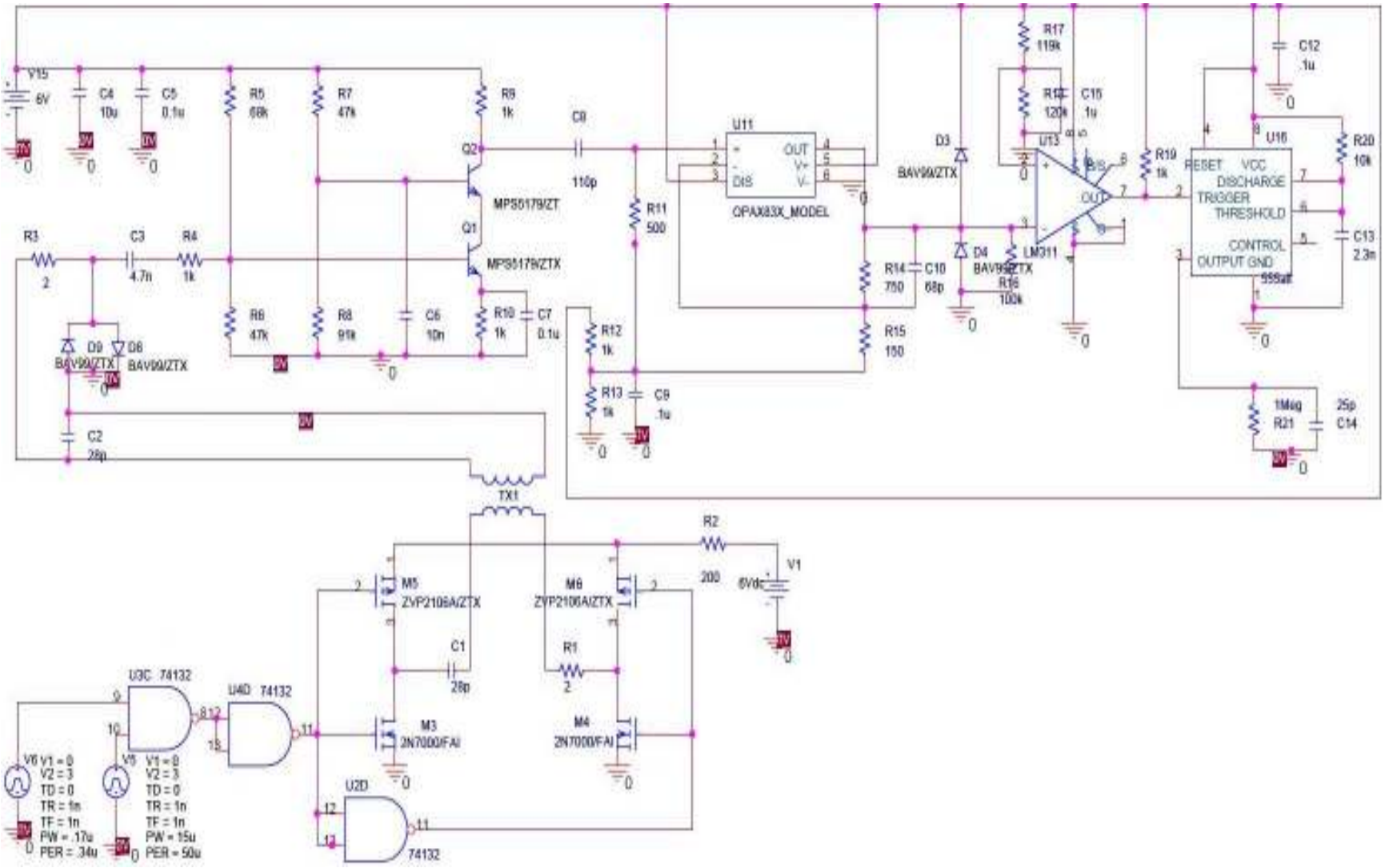

Figure 5. 3 MHz inductive link schematic.

C.1 Antenna Design

The original prototype used a pair of simple air core antennae; however, these antennae (specifically the transmitter antenna) were much too large for an ingestible pill system. In an effort to decrease the physical size of the antennae and increase their coupling factor, ferromagnetic cores were introduced. For a 3 MHz application, Fair-Rite Products Corporation manufactures open magnetic circuit antenna RFID rods made of a Nickel-Zinc composite ferromagnetic material, 61 (initial permeability of 125; suitable for 1 – 25 MHz applications) [57, 58]. The specific rod chosen as a core (part number 3061990911) [59] was selected because it had the largest radius available, 8 mm, while still small enough to fit in a prototype bolus pill. However, this material was very brittle, and attempts to reduce the original length of 45 mm using a Dremel tool were unsuccessful because it chipped very easily under the stress of power tools. As a result, a thin, fine tooth handsaw was needed to make length adjustments to the core material. Using this core material and number-of-turn equations provided by the manufacturer, a pair of 3.7 mH inductors were fashioned by wrapping 385 turns of 28 AWG (American Wire Gauge) magnetic wire in a single layer. Each inductor was then paired with a 28 pF capacitor in parallel with a 1 – 5 pF tuning capacitor whose value was adjusted until maximum coupling was achieved at a resonant frequency of 3 MHz.

C.2 Transmitter Design

The basic design of the 3 MHz transmitter, shown in Figure 6, remained similar to the prototype device, although a number of small changes were made. Figure 7 shows the functional block diagram for the transmitter.

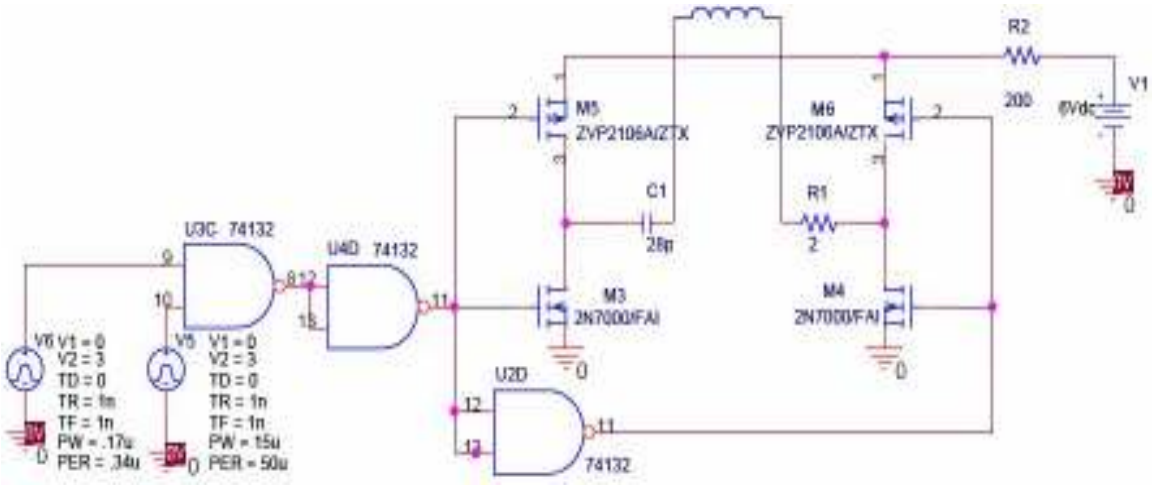

Figure 6. 3 MHz transmitter schematic.

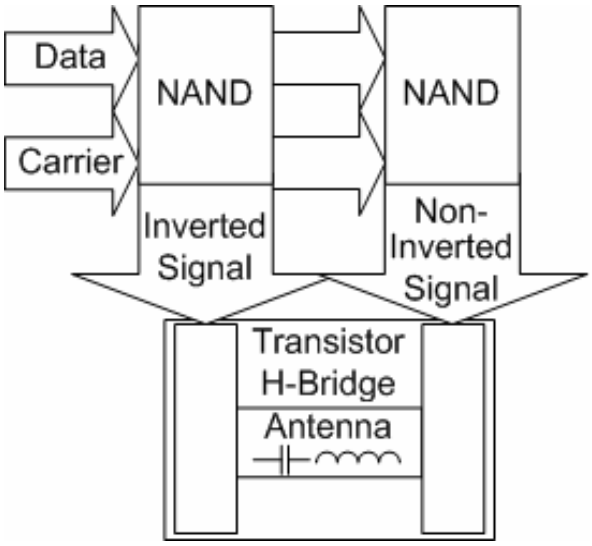

Figure 7. 3 MHz transmitter block diagram.

The biggest design change is that the original prototype operated at 3 V, but later designs have incorporated a 6 V power source. This will allow a larger voltage potential to be created across the transmitter antenna and in turn drive a larger current through the antenna. This design change also means that CMOS (Complimentary Metal Oxide Silicone), rather than TTL (Transistor-Transistor Logic), digital circuit components can be used in the design. There are a number of advantages of using CMOS rather than TTL components. First, CMOS at 6 V has a wider range of operating voltages (a larger supply noise margin). This allows a longer lifespan for an ingestible pill since a wider operating

voltage will allow a battery to be discharged more fully before a minimum usable threshold is reached. For example, a typical 3 V TTL chip (i.e., 74LS132N Schmidt trigger NAND gate) can effectively operate with a supply of 2.7 – 3.3 V (a supply noise margin of 300mV), while a typical CMOS chip (i.e., LMC555 CMOS timer) designed for 5 V can operate effectively with a supply of 3.5 – 12V (a supply noise margin of 1.5V, although the upper limit is increased significantly with CMOS logic). Second, CMOS devices use less power than their TTL equivalents since TTL devices continue to dissipate power in their zero state, while CMOS devices consume almost no power while in a zero state. CMOS devices also tend to be smaller than their TTL counterparts because TTL requires a greater number of transistors to accomplish the same task as the FETS used in CMOS devices [60]. Finally, CMOS devices tend to be cheaper primarily because they are in wider production.

Next, the carrier wave originally generated using a Schmidt Trigger NAND gate was instead supplied with an LMC555 timer circuit. While the timer circuit requires more secondary passive components (additional resistors and capacitors to tune the circuit), it generates a more consistent and reliable square wave with less noticeable rise and fall times associated with the dual threshold hysteresis action of the Schmidt trigger.

Finally, the prototype's half bridge was replaced with a full H-bridge. The implementation of this full H-bridge allows an even larger voltage drop, relative to a half bridge, to be applied across a load, which allows a greater current to pass through the inductive antenna, increasing the transmission distance.

C.3 Receiver Design

The receiver design for the 3 MHz prototype was a complete redesign of the proof of concept. Figure 8 shows the receiver schematic, while Figure 9 shows the block diagram of the receiver design.

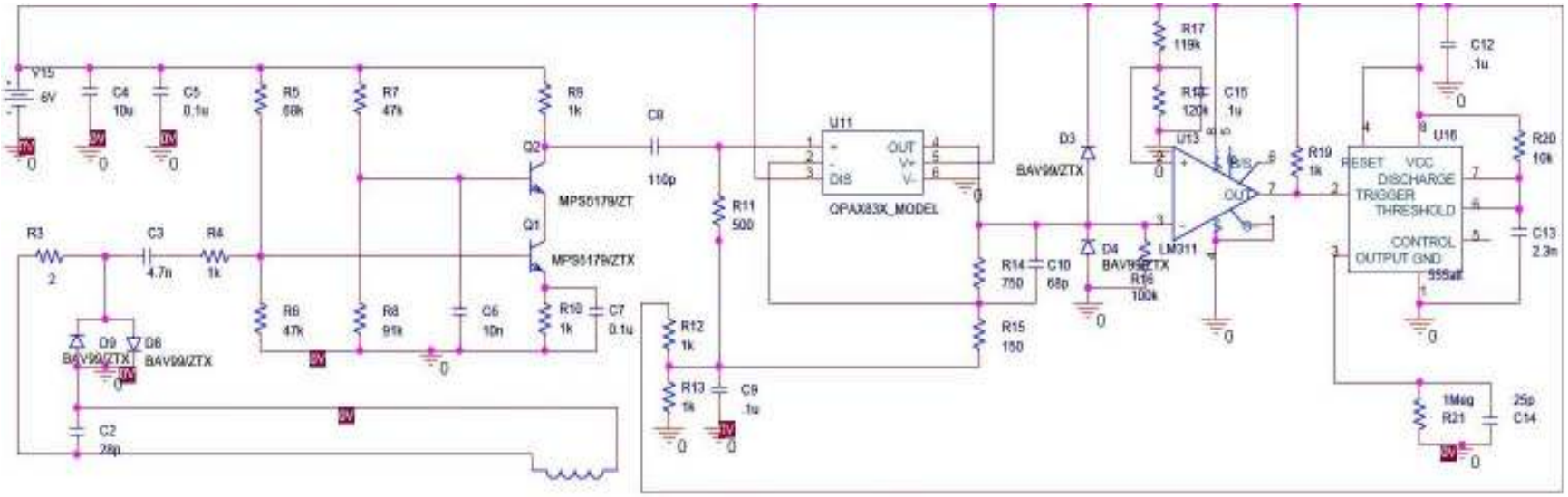

Figure 8. 3 MHz receiver schematic.

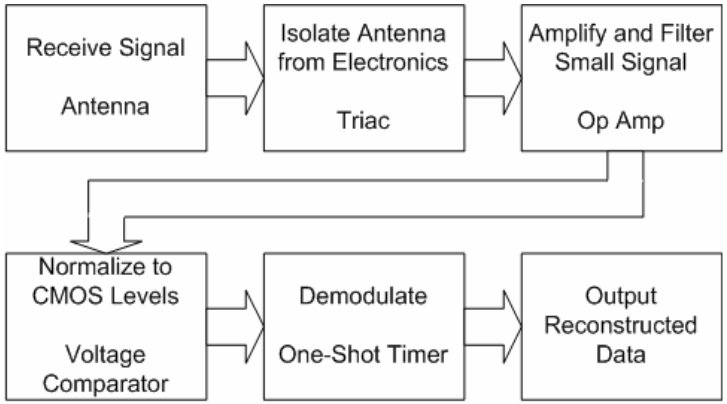

Figure 9. 3 MHz receiver block diagram.

While the first three stages are similar to the proof-of-concept design, they are implemented in different ways. The change to the antenna design has been already been discussed in this chapter. The next change was to remove the operational amplifier buffer and replace it with a triac. This was needed because the input impedance of the antenna became much larger (the frequency and inductance values were changed by an order of magnitude), such that a typical operational amplifier was no longer suitable to interface directly with the antenna. Without an operational amplifier in place to protect the transistors from the very large voltage spikes that can occur (especially when the transmitter is in very close proximity to the receiver), the triac (two anti-aligned diodes) was chosen to isolate the antenna from direct contact with the other electronics. The triac is positioned between the antenna and a transistor-based, cascoding preamplifier. While this preamplifier does add gain of its own, the primary purpose of the preamplifier is to convert a high impedance input (from the antenna) to a lower impedance output suitable for a match with an operational amplifier (or a multi-stage operational amplifier array) that can add much higher gain amplification compared to the preamplifier. While the original proof of concept used a cascading amplifier as its primary gain source, the cascoding design was chosen because it requires fewer components and consumes half as much power since the transistors are in series rather than parallel.

The implementation of the final step to reconstruct the original data is significantly different from the early design. Originally, the proof-of-concept design used a diode based rectifier and envelope detector to convert the AC, amplitude modulated signal to the DC data signal. However, the diode-based signal rectification and demodulation were abandoned in lieu of a voltage comparator (for DC rectification) paired with a one-shot trigger (for demodulation, based on LMC555's one-shot mode). The primary reason for this decision was that a diode, in order to form a rectifier, must be paired with a capacitor and resistor, which creates a non-trivial turn-on and turn-off time associated with the rectifier RC time constant, τ. This creates two separate time constants: one for the rectifier, τ_r, and one for the antenna, τ_a (due to the antenna's capacitor and magnetic wire with a non-zero resistance) which introduce unnecessary lag time and distort the reconstructed signal in comparison to the original signal.

DC rectification was completed by the diode, so a ripple would occur during the high state of the reconstructed data. This ripple manifests itself because each time the modulated signal changes from a high to low state, a discharge happens until the modulated signal goes back high. This means that special care had to be taken when choosing capacitor/resistor values to ensure that minimum discharge occurred between the high states of the modulated signal (at 3 MHz), while ensuring that the rectifier could be discharged in a timely manner with respect to the reconstructed data (at 20 kHz). For the rectifier to function on the 20 kHz data signal, some ripple would be present, which was removed via a voltage comparator to achieve a true DC rectification and also convert the signal to proper voltage levels.

The new design took a more modular approach to the rectification and demodulation processes, rather than having additional lag time between signal transitions and using a voltage comparator to clean up the signal created by the diode and envelope detector. First, DC rectification was accomplished with an OPA830 [61] connected to an LM311 high speed voltage comparator to convert the AC, amplitude modulated signal to a DC, amplitude modulated signal with a zero state at ground and a high state at Vcc. Then, demodulation was accomplished using an LMC555 timer as a one-shot trigger to extract the 20 kHz envelope from the modulated 3 MHz signal. The one-shot trigger in this design is a pulse based timing device with a single input and output that waits to turn on until a state transition is detected on the input, at which point its output turns on for a set period of time regardless of the input state. This means that the one-shot trigger will remain low until it encounters the first leg of a high state from the AM signal, at which point the one-shot trigger turns on for a period of 50 ns (1/20000 Hz) before returning to its low state. At this point, the data have been reconstructed to be an approximate match to the signal that was transmitted and can be ported to a pin to connect to whatever electronics interface is available (whether it be the current BMOO prototype, a future mote based system, or a link tester).

C.4 Results

The initial design required some revisions. When the transmitter and receiver shared a common ground or power line, the results seemed much more encouraging in simulation than in reality. Obviously, if the transmitter, receiver, and oscilloscope were powered from the same power supply, they would share both the ground and power lines. In this case, if the receiver output was tracked with the oscilloscope, the probe's ground line would hold some crosstalk from the transmitter mixed with the actual signal from the receiver, making the signal detected by the receiver appear overly large. Less obviously, if the transmitter, receiver, and oscilloscope were on separate power supplies, but the supplies shared a common ground (such as a building's ground line), this phenomenon would still be observed. Initial testing was done with HP plug-in power supplies in a laboratory environment where all the power in the room shares a common ground. That being the case, this phenomenon was not observed until the prototype link was run on battery power (where the transmitter, receiver and oscilloscope had completely independent ground and power lines). The initial conclusion was that running off of AA batteries might pose a problem (i.e., AA batteries may be unable to provide enough current for the transmitter). However, after further investigation, the battery type did not seem to be the problem, since it was observed that a disconnected probe would still show an inkling of the transmitted signal when the transmitter was run from a power supply in the same room (but not when the transmitter was on battery power). As a result, many layers of decoupling capacitors were added to both the transmitter and receiver, not just between an individual component's power and ground, but also anywhere a signal was output from one component to another. Also, since the transmitter requires few components, a double layer prototyping board was used, with the bottom half acting as a ground plane and the top half being used to surface mount the components. While a similar approach was not feasible for the prototype receiver (since there are many more components and line paths), future revisions using smaller PCB designs should incorporate this idea for both the transmitter and receiver. Figure 10 - Figure 12 show some example signals acquired with an Agilent oscilloscope with both the transmitter and receiver on battery power at a separation distance of 12 inches with the transmitter submerged in a saline solution.

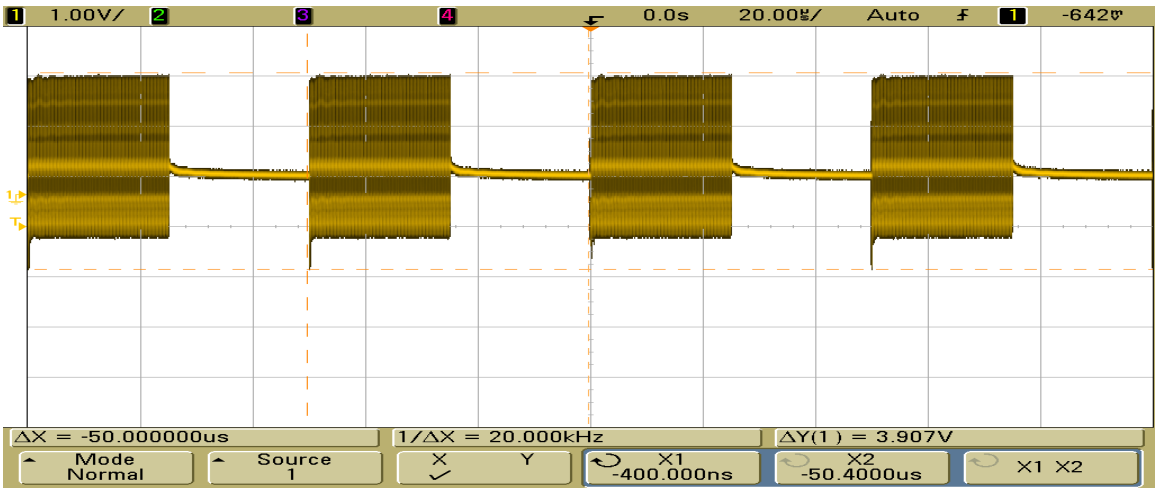

Figure 10. 3 MHz transmitter antenna output.

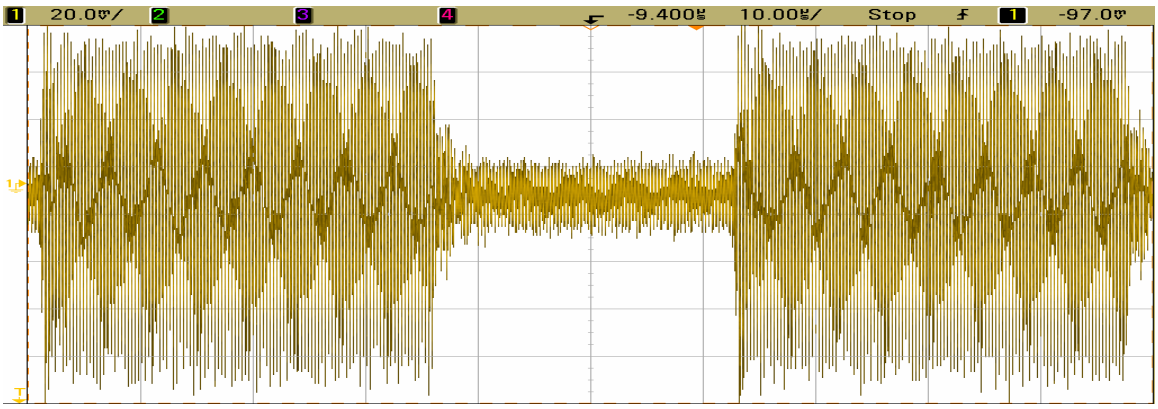

Figure 11. 3 MHz receiver direct antenna input

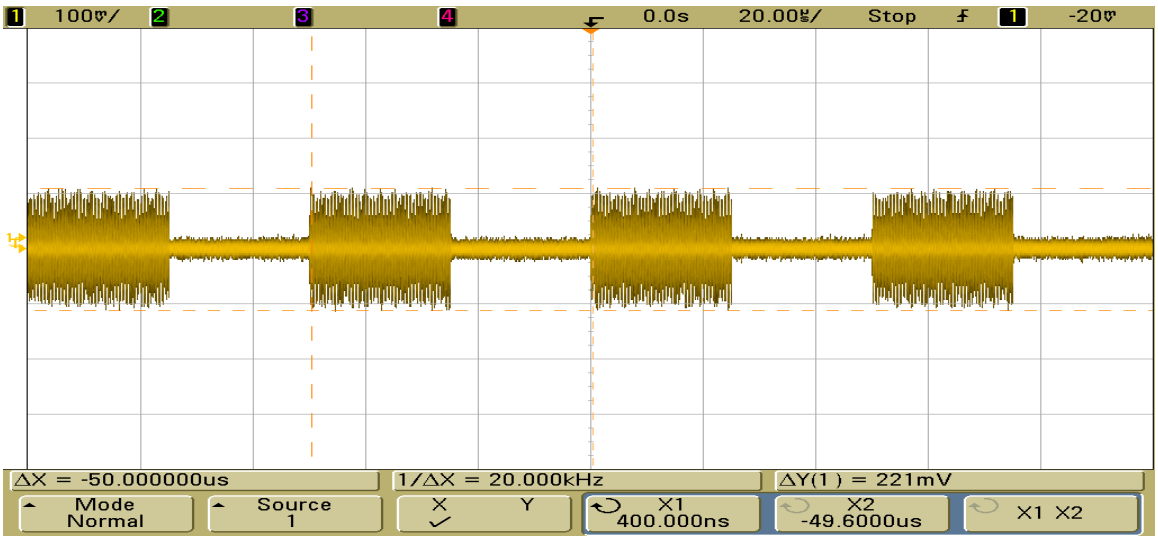

Figure 12. 3 MHz receiver amplified data stream.

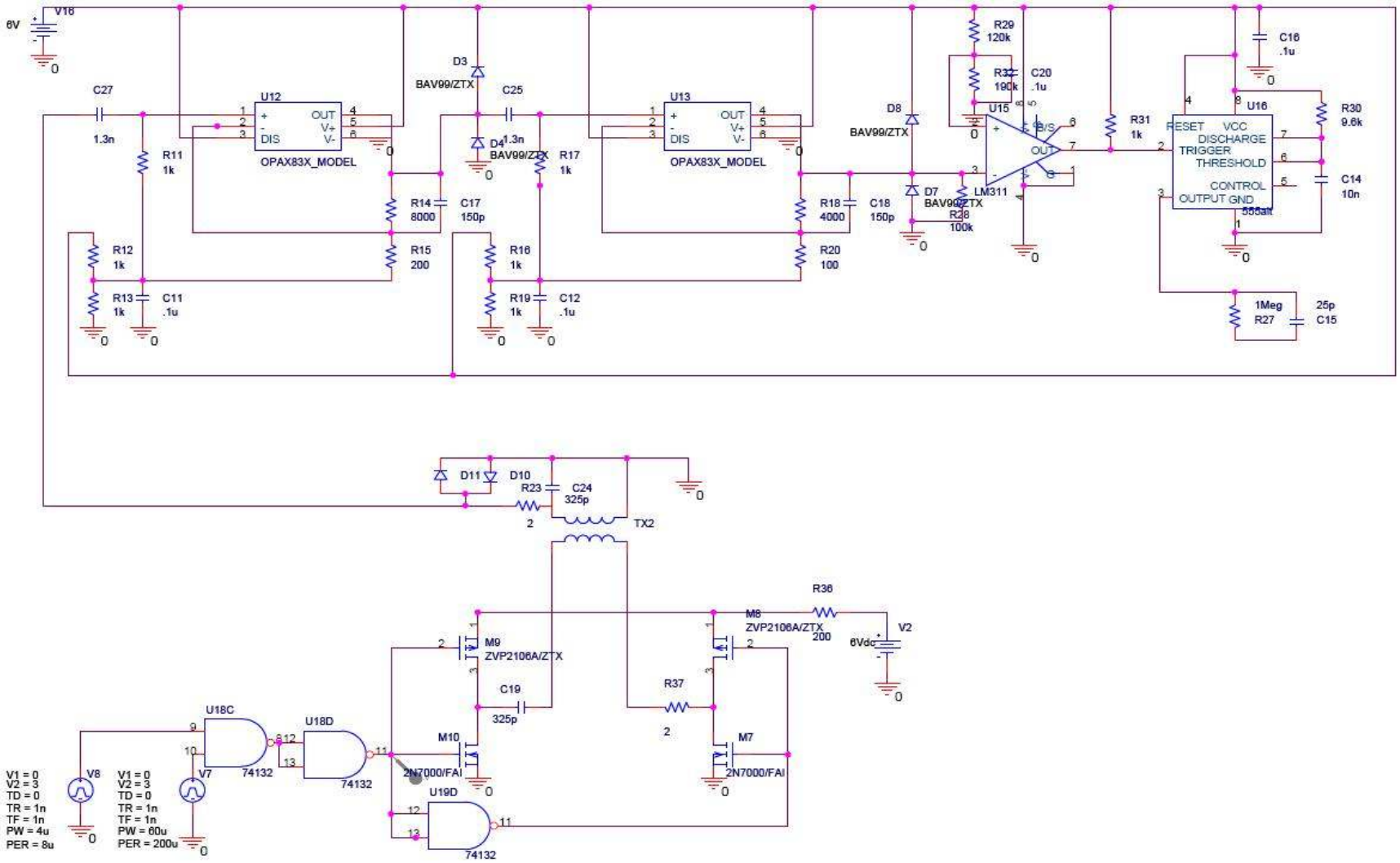

Figure 13. 125 kHz inductive link schematic.

D. 125 kHz Prototype Design

The 3 MHz design was an improvement relative to the original proof of concept, but more room for improvement remained. The operable distance was increased nearly tenfold to ten to fifteen inches, while the physical dimensions of the antennae were reduced greatly, but this distance was still inadequate to reliably transmit from the stomach to, e.g., the neck of a full-grown steer, a distance that may be up to three feet. Additionally, 3 MHz is not a standard operating frequency for commercial devices in this field. In an effort to appeal to a standard commercial frequency for this type of application [54, 55] and further increase transmission range, a new design was needed to operate at 125 kHz. Figure 13 shows the schematic of the entire system design including the transmitter, the receiver, and their antennae. These schematics are also available in Appendix B along with board layouts and parts lists.

D.1 Antennae Design

The design approach was similar to the approach used for the 3 MHz prototype. However, a different core material was needed to operate at the new frequency. An open magnetic circuit antenna RFID rod was again chosen from Fair-Rite Products Corp. This time the material was a Manganese-Zinc composite ferromagnetic material, 78 (initial permeability of 2300; suitable for up to 200 kHz) [62]. This material proved less brittle and provided a larger permeability than the Nickel-Zinc material. The largest diameter rod was chosen (part number 3078990911), and this time the length was successfully shortened to 25 mm by cutting the rod with a Dremel tool. However, since the carrier frequency was now an order of magnitude smaller, much larger L and C values were needed (5 mH and 324 pF, respectively). This meant that inductor construction was achieved by means of a multiple wire-turn layers. A larger L value with multiple layers added difficulty in calculating the exact number of turns and layers needed, and it introduced complex interactions between the wire layers. However, this configuration had the benefit of increasing the radius of the antennae for each layer used. In the end, each inductor was wound with approximately 700 total turns in 7 layers with about 100 turns per layer. A larger C value also added some difficulty because a small tuning capacitor was no longer adequate to cover the range of possible values. Instead, each

inductor was connected to an HP 4342A Q-meter to find the exact capacitance needed to achieve the desired resonant frequency of 125 kHz.

D.2 Transmitter Design

Figure 14 shows the schematic for the inductive transmitter operating at 125 kHz. The transmitter design remained largely unchanged from the previous prototype. The only difference regards the capacitor and resistor values connected to the LMC555 timer to achieve the new carrier frequency. In fact, the exact same transmitter was repurposed for the new prototype, with new components soldered in place of the previous values.

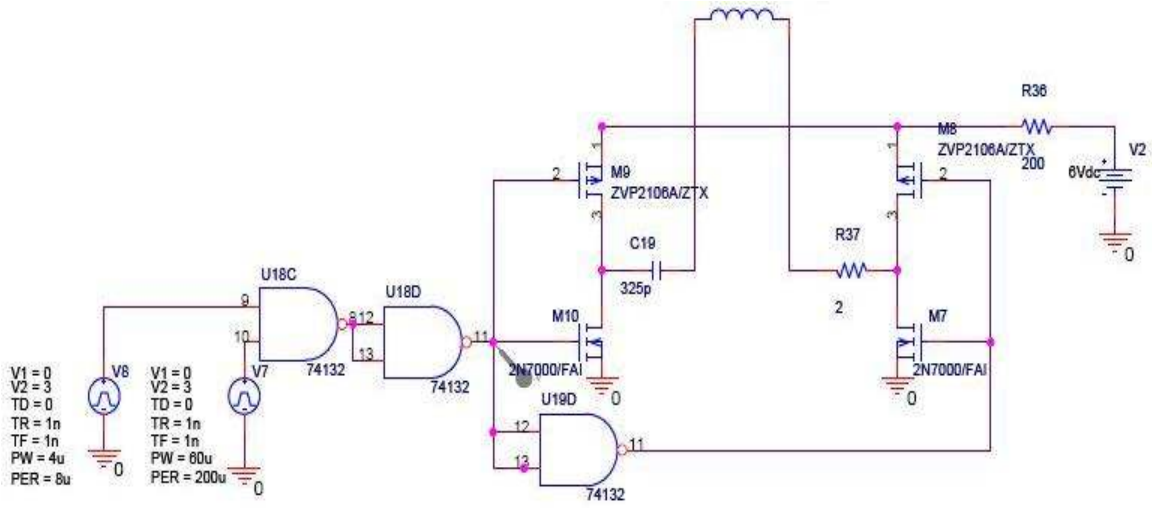

Figure 14. 125 kHz transmitter schematic.

D.3 Receiver Design

Figure 15 shows the schematic for the 125 kHz inductive receiver, which required relatively more redesign than the 125 kHz transmitter. First, with this design, the impedance of the antenna was significantly reduced such that a preamp was no longer necessary, so the antenna could interface directly with an operational amplifier circuit. That being the case, two stages of amplification were used: one that replaced the preamplifier and a second stage of additional gain.

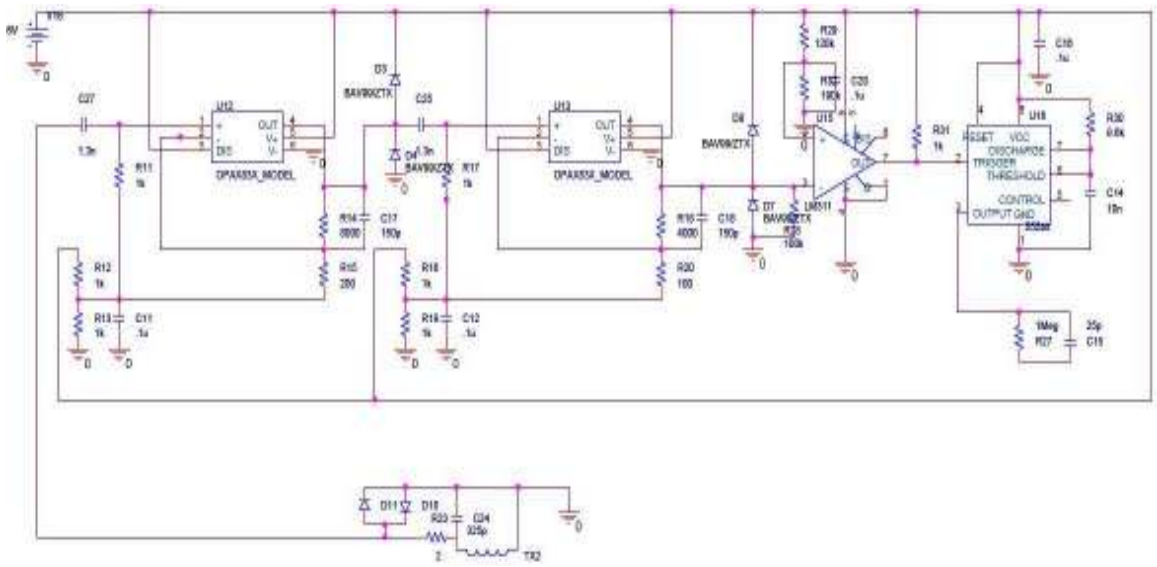

Figure 15. 125 kHz receiver schematic.

D.4 Results

This final design iteration was the best performing inductive link to date. Figure 16 shows the signal at various circuit positions, where the transmitter-to-receiver antenna distance was about 20 inches and the transmitter was submerged in a bucket of saline solution approximating tissue. The top two traces are the original binary data (DATA) created by an auxiliary LMC555 timer and the modulated data (MOD) resulting from the inverted NAND of the 20 kHz data with a 125 kHz carrier wave. The lower two traces are the signals across the transmitting antenna (TX) and the receiving antenna (RX).

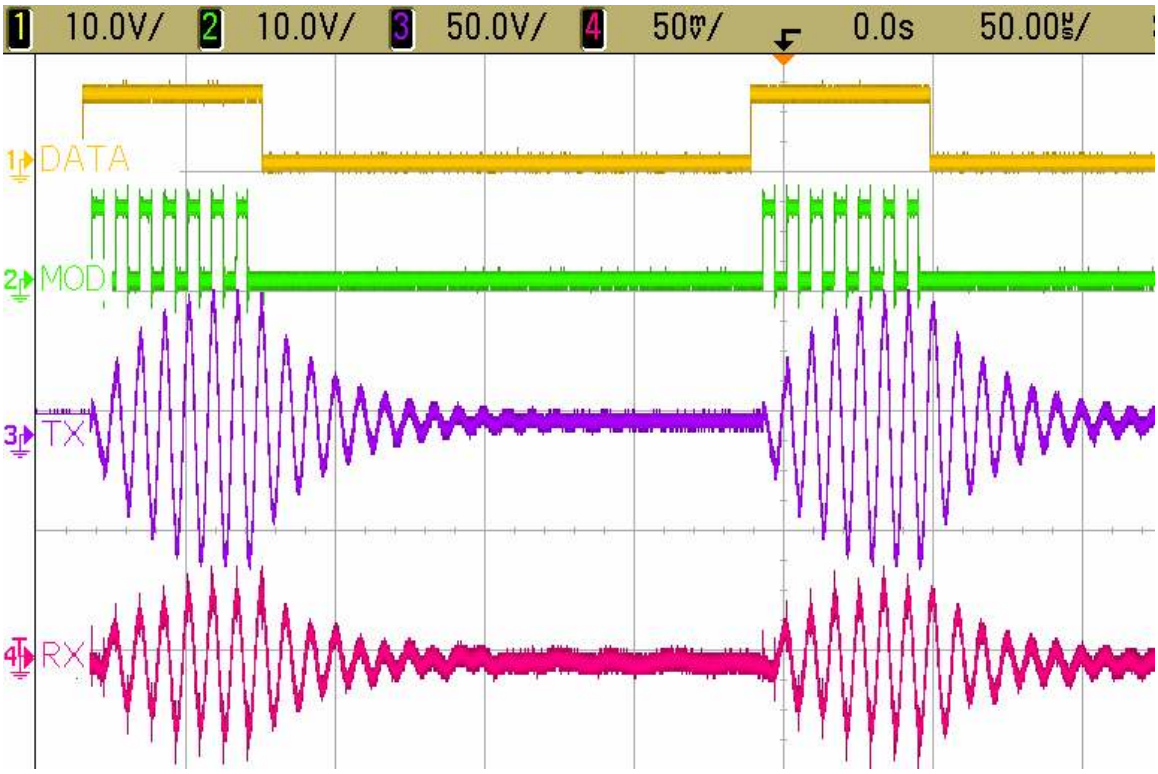

Figure 16. 125kHz Inductive link data traces.

E. Future Improvements

Inductive communication through the body of a cow was proven feasible with minimal signal attenuation occurring compared to free air transmission. While an ideal transmission range was not achieved for ear tag devices, belt-mounted systems are feasible. However, in addition to pushing the limits of transmission range as far as possible, there is still much to be done to have an ideal inductive communication link fully integrated in the BMOO system.

The current prototype is a hand-soldered device built on a through-hole protoboard. This means that the electronics are much larger than necessary, so a transition to a printed circuit board (PCB) is the next natural step. However, this step would best be accomplished in unison with the PCB design of the bolus since these components need to be interfaced together in such a way that they fit in a pill form factor. An ideal situation would be to create this on a single PCB, although they could be made as separate modules as long as proper considerations were taken.

Next, integration work is needed to merge the inductive link with the sensor electronics in order to transfer these data from the internal sensors to the external BMOO unit. The current bolus prototype streams data directly to a data acquisition card on a laptop computer. A connection needs to be established between the bolus and inductive link, preferably with a temporary means of storage in the case of an inductive link failure. Also, before the data are passed to the inductive link for transmission to the outside world, some sort of packet structure (and means of encapsulation/decapsulation) needs to be developed. This packet structure can either be derived from the existing BMOO packet structure [3, 4] or from the standards for 125 kHz LF RFID communication [55], but it needs to include at least a timestamp, unique identification number, and checksum. Currently, the prototype has been tested with raw binary data (typically square waves), but real data will need to be encoded for transmission. An ideal coding scheme would be one that that incorporates error detection and correction. However, the current version of the inductive link can only provide one-way communication (from the internal transmitter to the external receiver). Two-way communication is preferred because it allows more robust error handling. With one-way communication, when the receiver obtains new data, there is no way to signal the transmitter that reception was successful. This means that if an error is detected, a software algorithm would need to correct the data rather than request retransmission. A two-way communication scheme would mean an improvement to the current inductive prototype. This would require combining the transmitter and receiver into a single transceiver with two separate transmission lines (Rx and Tx). An inductive transceiver would likely require two separate antennae operating at different frequencies whose signal and signal harmonics do not overlap (to avoid collisions and crosstalk)

The current prototype is also highly directional. One way to resolve the directionality issue would be to make a transmission module that has three antennae arranged perpendicularly (and orthogonally) on each axis of three-dimensional space. Unfortunately, this would require separate driving electronics for each antenna, resulting in triple the board space and power requirements compared to the current inductive link.

If this idea were combined with implementing a transceiver, this would mean each transceiver would require four antennae (three for transmission and one for reception) and two frequencies (one for Rx and one for Tx).

Finally, if all of these improvements were made, battery life would become a more pressing issue than it is now. A possible solution would be wireless power transmission from the external (more accessible) device to the internal device. There are solutions that exist to provide both data and power over a single link [37, 42]. This would be a desirable solution in itself because it would allow a sensor pill to have an indefinite lifespan. The cost of implementing a monitoring device such as this could be more justifiable to a livestock rancher if a single sensor pill could be active for the entire lifetime of an animal without the need to change batteries.

CHAPTER 6: CONCLUSIONS

A physiological sensor network designed to continuously monitor cattle health would be enormously beneficial to both the livestock industry and the general public. Meat quality, production cost, and safety are of utmost concern and depend heavily on the well-being of individual animals. Overall herd health is also dependent on the ability to segregate sick animals from the herd once an illness is detected. The ability to identify illness onset traditionally relies on visual inspection and on-site veterinary visits, but this identification and segregation process could be expedited by outfitting individual animals with near real-time tracking and monitoring systems.

BMOO project collaborators have identified a number of data metrics that can provide insight into animal well-being: core temperature, heart rate, respiration rate, rumen pH, activity, animal location, and ambient temperature/humidity, to name a few. The team has demonstrated the ability to acquire and store many of these data metrics through the use of an array of sensors coupled with an aggregate storage system. Some of these sensors can be practically worn on the outside of the animals (e.g., accelerometers, ambient sensors, and GPS locators), but the team has generally concluded that vital information is best acquired from sensors inside the animal if possible. Internal sensors facilitate a protected and consistent sensing environment but also create design challenges in terms of wireless data transmission from the inside of an animal to an outside receiver. In the mean time, progress has been made to develop novel multi-dimensional sensor pills that rely on wired technology and the availability of fistulated animals that offer rumen and reticulum access.

While wireless communication is a necessity, conventional radio-frequency communication technology is ill-suited for use with internally placed sensors in large animals because the interaction of propagating waves with water based tissue leads to extreme signal attenuation, resulting in data loss. Therefore, a suitable alternative wireless technology, near-field inductive communication, has been investigated and found to be less prone to signal decay in tissue. An inductive communication link creates

a quasi-static magnetic field of controlled, dynamically modulated data signals. In addition, near-field communication devices consume less power and require less physical space than typical radio communication devices, making them ideal for internally placed sensors.

The research summarized in this thesis has demonstrated the viability of near-field communication for this domain but has also demonstrated shortcomings of the technology. While signal attenuation through a biological medium is not as drastic as with radio waves, inductive antennae are highly directional. This poses problems for coherent communications when the transmitting antenna is inaccessible, such as with internal sensors that reside in a swallowable pill. This implies a need for three-dimensional antennae that may take up more space and require more power. Further, a useful inductive communication link may require two-way communication so that errors can be identified and the associated data can be retransmitted. This would come at the cost of antenna complexity, power draw, and space allocation. Such extra cost does not counteract the benefits of using near-field communication instead of radio communication, but it is not ideal for use in a sensor pill that already has space constraints driven by the presence of multiple sensors, storage, and battery power.

Finally, near-field designs are sensitive to minor source noise. Accurately prototyping near-field communication devices on socket (solderless) breadboards proved nearly impossible due to the effects of the additional capacitance and signal paths on the intended signals. Even soldered protoboards require a great deal of decoupling and attention to trace lines, ground paths, and solder mass to avoid the introduction of disruptive noise. Ideally, future versions will be implemented directly on machine-made PCB boards with smaller components and trace routes to reduce noise and improve throughput and transmission distance.

REFERENCES

[1] Cattlemen's Beef Board and National Cattlemen's Beef Association. "Beef Market at a Glance Fact Sheet," The Beef Checkoff, 2009.

[2] U. S. Department of Agriculture. "NAIS - The National Animal Identification System," vol. 2008: United States Department of Agriculture, http://animalid.aphis.usda.gov/nais.

[3] L. J. Nagl. "The Design and Implementation of a Cattle Health Monitoring System," *Electrical Engineering*: Kansas State University, 2000.

[4] D. Gélinas. "Bovine Modile Observaion Operation Device Software Engineering Report," Kansas State University, 2003.

[5] Analog Devices. "ADXL210E Low-Cost +/-10*g* Dual-Axis Accelerometer with Duty Cycle," 2002, http://www.analog.com/static/imported-files/data_sheets/ADXL210E.pdf.

[6] Trimble Navigation Limited. "Lassen SQ GPS Receiver System Designer Reference Manual," 2004.

[7] HQI Inc. "CoreTemp Core Body Temperature Monitoring System User Manual," 2004,

[8] Zigbee Alliance. "ZigBee Specification," 2006,

[9] R. Lourens and I. Microchip Technology. "Low Frequency Magnetic Transmitter Design," 2002, http://ww1.microchip.com/downloads/en/AppNotes/00232a.pdf.

[10] TERN Inc. "FlashCore-B Technical Manual," 2003, http://www.tern.com/portal/library/fb.pdf.

[11] CompactFlash. Association. "CompactFlash Specification," 1994-2010, http://www.compactflash.org.

[12] Microchip Technology Inc. "PIC18F2525/2620/4525/4620 Data Sheet," http://ww1.microchip.com/downloads/en/DeviceDoc/39626b.pdf.

[13] Microchip Technology Inc. "PICDEM Z Demonstration Kit User's Guide," 2004, http://ww1.microchip.com/downloads/en/devicedoc/51524a.pdf.

[14] Dallas Semiconductors Maxim IC. "DS1337 Real-Time Clock Datasheet," 2008.

[15] Maxim. "Microprocessor Supervisory Circuits MAX690-MAX695," 2005.

[16] Texas Instruments. "ULTRA-LOW QUIESCIENT CURRENT 150-mA LOW-DROPOUT VOLTAGE REGULATORS Datasheet," 1999.

[17] Paradigm Systems. "Paradigm C++ Professional IDE," 2006, http://www.devtools.com/pcpp/ide.htm.

[18] Trimble Navigation Limited. "Differential GPS Beacon TSIP," pp.

[19] National Marine Electronics Associations. "NMEA 0183 Standard," 2003, http://www.nmea.org/content/nmea_standards/nmea_083_v_400.asp.

[20] K. D. Smith. "A Wearable Cattle Health Monitoring System with an Emphasis on Motion-Based Behavior Assessment," *Electrical Engineering*: Kansas State University, 2004.

[21] Sensirion. "Datasheet SHT1x Humidity and Temperature Sensor," 2006.

[22] A. M. Martinez. "Acquisition of Heart Rate and Core Body Temperature in Cattle Using Ingestible Sensors," *Electrical Engineering*: Kansas State University, 2005.
[23] Polar Electro USA. "Polar," 2006, http://www.polarusa.com.
[24] Maxim IC Products. "MAX3233E, MAX3235E ±15kV ESD-Protected, 1µA, 250kbps, 3.3V/5V, Dual RS-232 Transceivers with Internal Capacitors ", 2004.
[25] Digital Angel. "Digital Angel Biothermal System," 2006, http://www.digitalangel.com.
[26] A. Tomek. "USDA Approves Digital Angel's RFID Chip for Equine use in National Animal Identification System," Digital Angel Corporation, 2007, http://www.digitalangel.com/press_details.aspx?F=20070904.htm.
[27] Texas Instruments. "2.4 GHz IEEE 802.15.4 / ZigBee-ready RF Transceiver," 2008.
[28] IEEE Computer Society. "Wireless Medium Access Control (MAC) and Physical Layer (PHY) Specifications for Low-Rate Wireless Personal Area Networks (WPANs)," 2007.
[29] D. Lattibeaudiere. "Application Note 1232, Microchip Zigbee 2006 Residential Stack Protocol," Version 2.0-2.6 ed, 2008, http://ww1.microchip.com/downloads/en/AppNotes/ZigBee2006%20Application%20Note%20AN1232A.pdf.
[30] N. Rajbharti. "Application Note 965(a), Microchip Stack for the ZigBee Protocol," Version 1.0-3.4 ed, 2004, http://ww1.microchip.com/downloads/en/AppNotes/00965a.pdf.
[31] D. R. B. Reese. "A Zigbee subset/IEEE 802.15.4 Multi-platform Protocol Stack," 2007, http://www.ece.msstate.edu/~reese/msstatePAN/msstate_lrwpan_doc_release.pdf.
[32] Crossbow Technology. Inc. "Mica2 Wireless Measurement System Datasheet"
[33] Erik A. Johannessen, Tong Boon Tang, Lei Wang, Alexander Astaras, Mansour Ahmadian, Li Cui, Alan F. Murray, Jonathan M. Cooper, Steve P. Beaumont, Brian W. Flynn, David R. S. Cumming. "IDEAS: A miniature lab-on-pill multisensor," *IEEE NORCHIP 2002*. Copenhagen, Denmark: IEEE, 2002,
[34] Lei Wang, Erik A. Johannessen, Cathy Wyse, David R. S. Cumming, and Jon M. Cooper. "Biocompatibility of a Lab-on-a-Pill Sensor in Artificial Gastrointestinal Environments," *IEEE Transactions on Biomedical Engineering*, vol. 53, no. 11.
[35] Jia-Jen J. Chen. Chih-Kuo Liang, Cho-Liang Chung, Chen-Li Cheng, and Chua-Chin Wang. "An implantable bi-directional wireless transmission system for transcutaneous biological signal recording," *Physiological Measurement*, pp., January 2005.
[36] G. Horler and S. Couchman. "Inductively Coupled Telemetry and Actuation," IEE Seminar on Telemetry and Telematics, April 2005.

[37] M. S. Douglas C. Galbraith, and Robert L. White. "A Wide-Band Efficient Inductive Transdennal Power and Data Link with Coupling Insensitive Gain," *IEEE TRANSACTIONS ON BIOMEDICAL ENGINEERING*, vol. BME-34, no. 4, pp. 265-275.
[38] G. Meron, Gavriel Iddan, Arkady Glukhovsky, Paul Swain. "Wireless Capsule Endoscopy," *Nature*, vol. 405.
[39] T. D. Drysdale, Lei Wang, and D. R.S. Cumming. "In Situ Characterization of Two Wireless Transmission Schemes for Ingestible Capsules," *IEEE Transactions on Biomedical Engineering*, vol. 54, no. 11, pp., November 2007.
[40] B. W. Flynn, M. Ahmadian, A.F. Murray, and D.R.S Cumming. "Data transmission for implantable microsystems using magnetic coupling," *IEEE Proceedings on Communications*, vol. 152, no. 2, pp., April 2005.
[41] R. S. Mackay. "Radio Telemetering from within the Body," *Science*, vol. 134, pp. 1196-1202, 1961.
[42] D. A. DeMichele and P.R. Troyk. "Inductively-Coupled Power and Data Link for Neural Prostheses using a Class-E Oscillator and FSK Modulation," 25th Annual International Conference of the IEEE EMBS, Cancun, Mexico, September 17-21, 2003.
[43] S. Birrer, R. Benedetti, P.A. Neukomm. "Overview of Telemetry Systems with Inductive Links and Variable Coupling Distances," March 1995, 1995.
[44] F. A. Miranda, R. N. Simons, J. D. Wilson, and R. E. Simons. "Wearable Wireless Telemety System for Implantable BIO-MEMS Sensors," 28th Annual EMBS International Conference, August - September 2006.
[45] P. Swain. "Wireless Capsule Endoscopy," *Gastrointestinal Endoscopy*"
[46] J. Wang. "A Novel Magnetic Communication System for WIreless Transmission Operating at 14.9MHz"
[47] D. V. K. Zworykin. "A Radio Pill," *Nature*, vol. 179, pp. 898, 1957.
[48] St. Jude Medical. "Accent DR RF Dual-Chamber Pacemaker Specification Sheet," 2009.
[49] Microchip Technology Inc. "microID™ 13.56 MHz RFID System Design Guide"
[50] Microchip Technology Inc. "microID™ 125 kHz RFID System Design Guide," 1998.
[51] C. R. Paul. *Electromagnetics for Engineers*: Wiley, 2004.
[52] M. N. O. Sadiku. *Elements of Electromagnetics*, Third ed: Oxford University Press, 2001.
[53] Fair-Rite Products Corp. "Fair-Rite Products Catalog," 2009, http://www.fair-rite.com.
[54] International Organization of Standardization. "ISO 11785: Radio Frequency Identification of Animals - Technical Concepts," 1996.
[55] International Organization of Standardization. "ISO 11784: Radio Frequency Identification of Animals - Code Structure," 1996.
[56] ON Semiconductor. "Quad 2−Input NAND Gate with Schmitt−Trigger Inputs High−Performance Silicon−Gate CMOS Datasheet"

[57] Fair-Rite Products Corp. "Material 61," 2007, http://www.fair-rite.com/newfair/materials61.htm.
[58] Fair-Rite Products Corp. "Soft Ferrite Component 61 Material Safety Data Sheet," 2005.
[59] Fair-Rite Products Corp. "Fair-Rite Antenna/RFID Rods"
[60] J. M. Rabaey. *Digital Integrated Circuits*, Second ed: Prentice Hall, 2003.
[61] Texas Instruments. "OPA830 - Low-Power, Single-Supply, Wideband Operational Amplifier"
[62] Fair-Rite Products Corp. "Material 78," 2007, http://www.fair-rite.com/newfair/materials78.htm.

APPENDIX A : BMOO UNIT SCHEMATICS

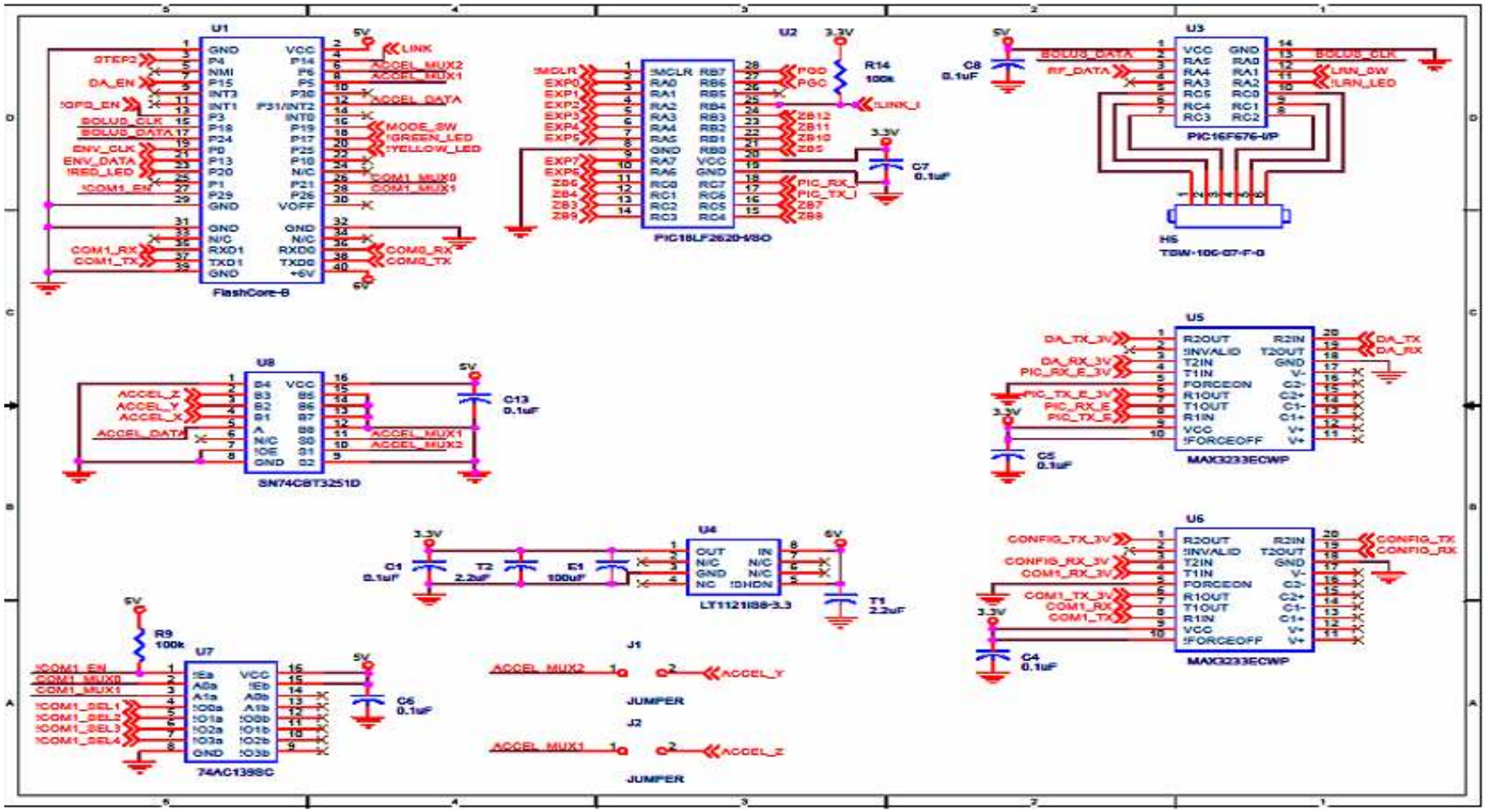

Figure 17. BMOO unit schematics page 1 – microcontrollers.

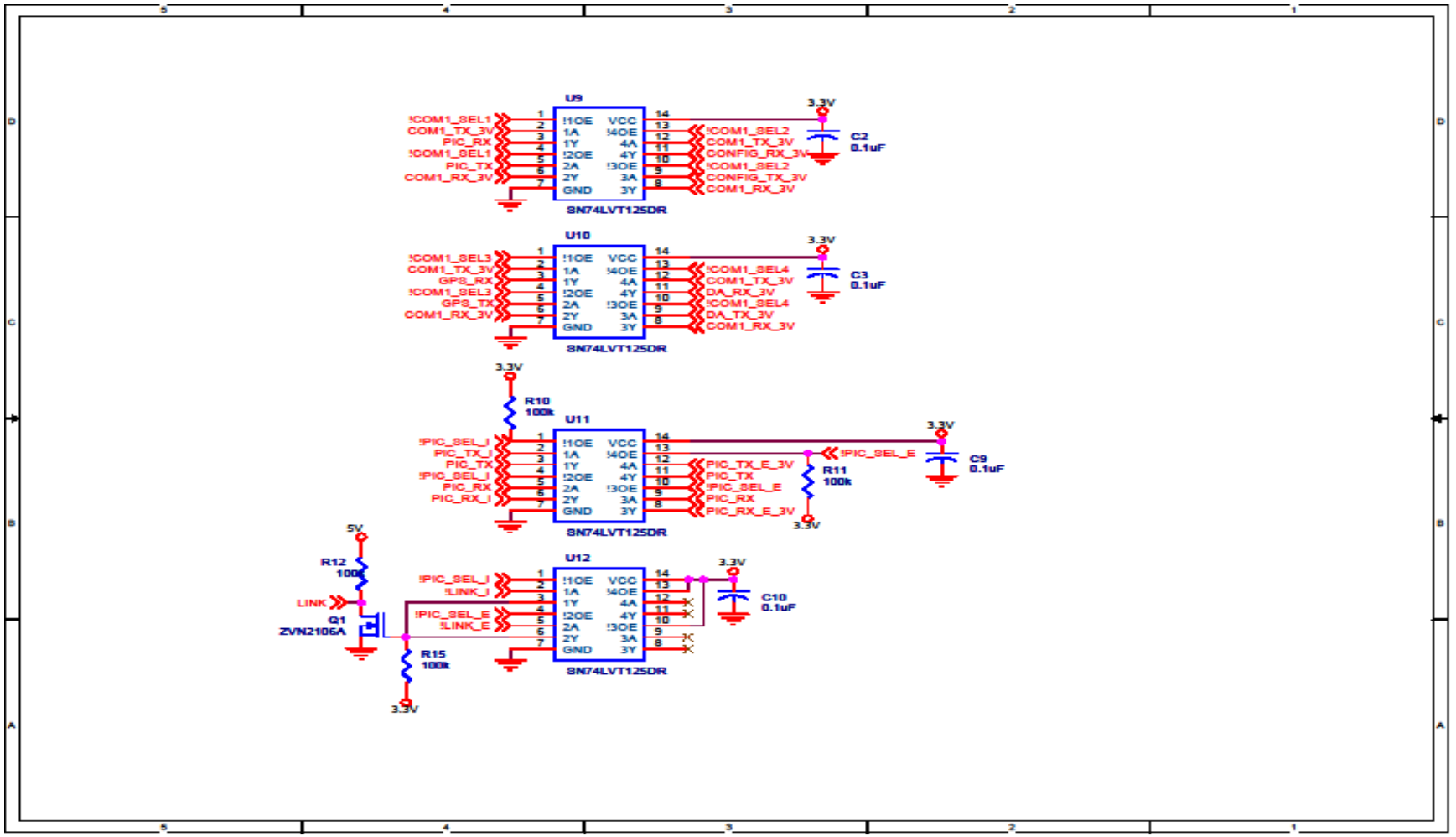

Figure 18. BMOO unit schematics page 2 – line drivers and buffers.

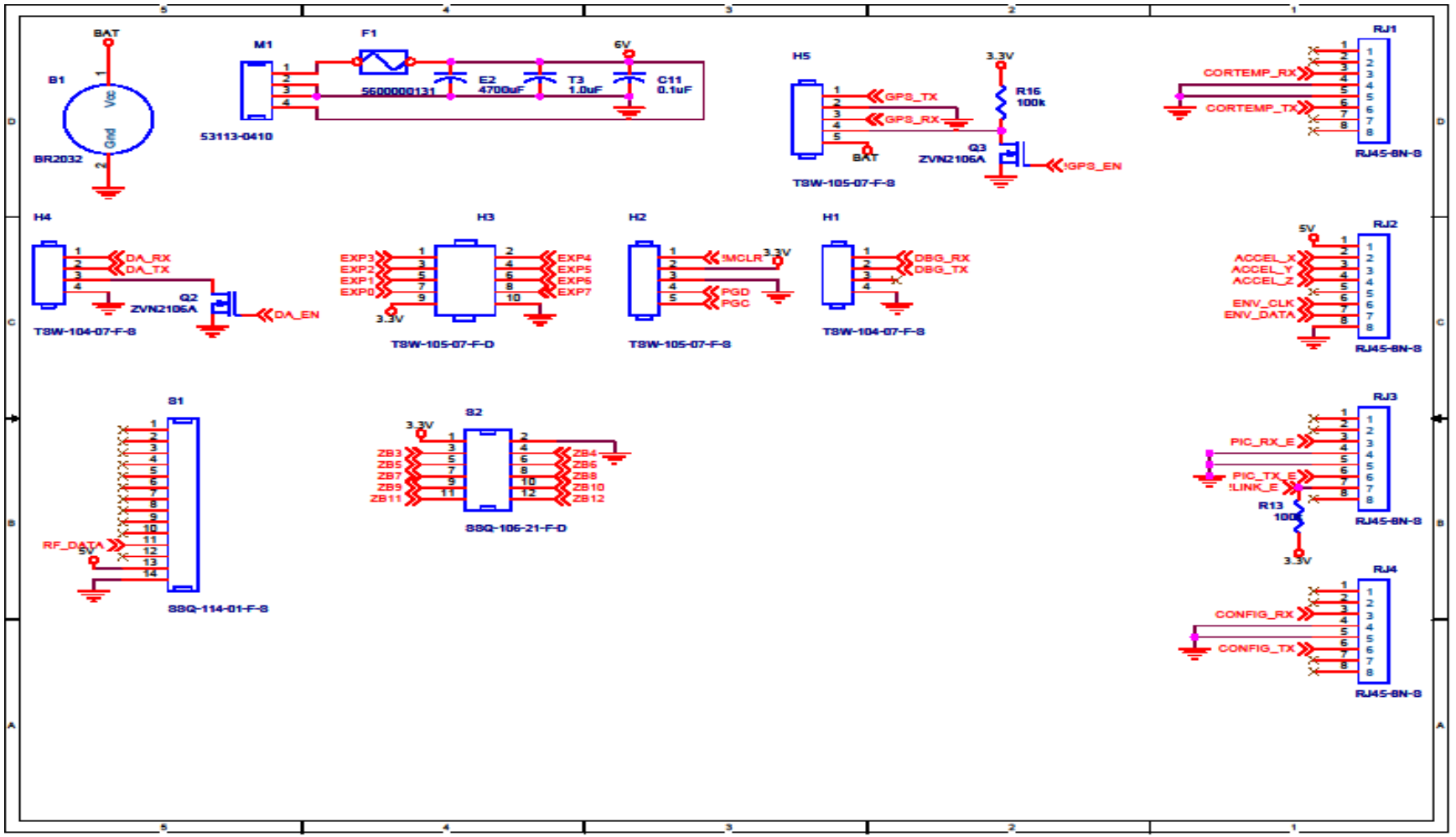

Figure 19. BMOO unit schematics page 3 – power and data connections.

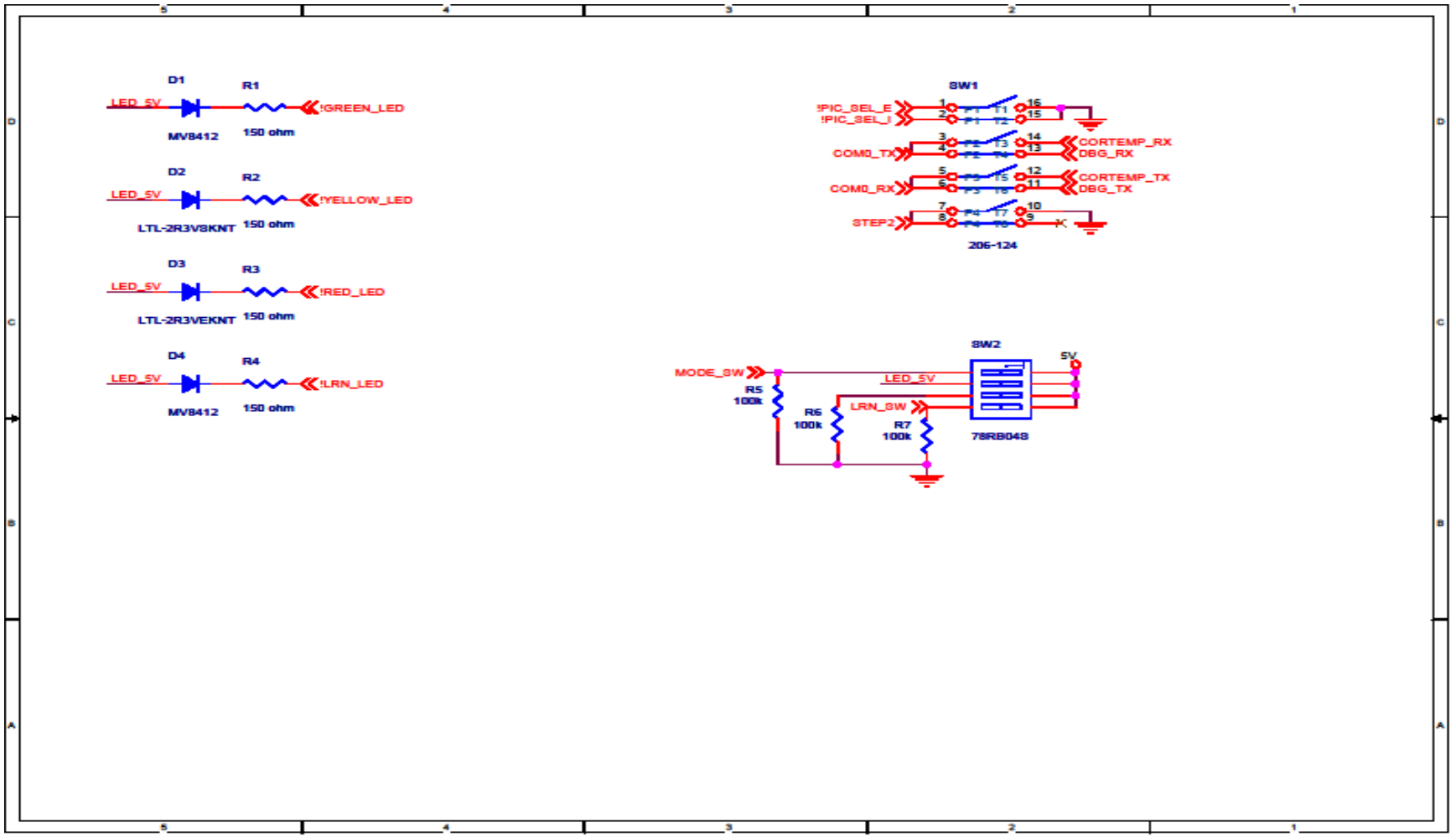

Figure 20. BMOO unit schematics page 4 – user interaction (switches, DIPs, LEDs).

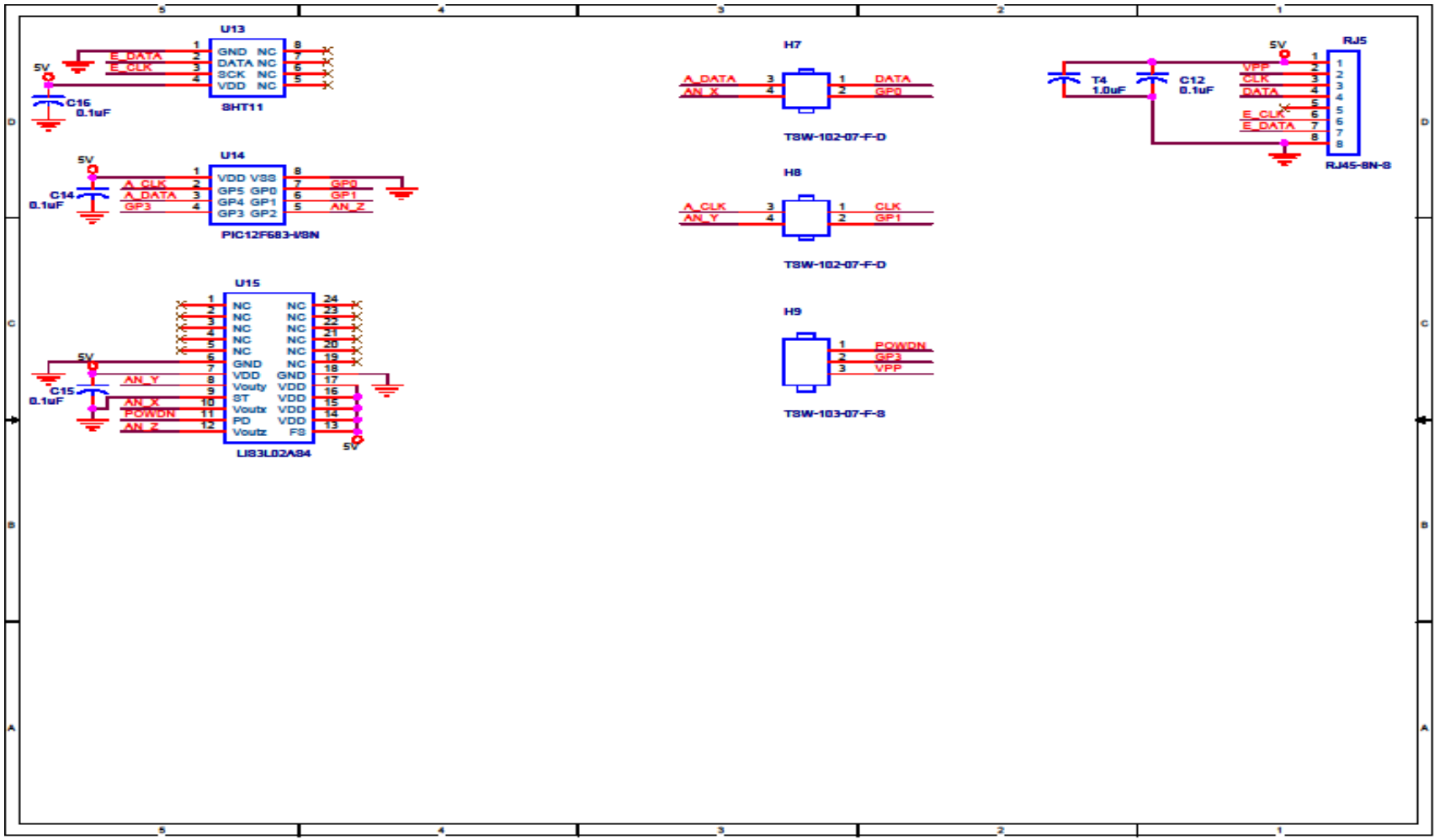

Figure 21. BMOO unit schematics page 5 – sensor and data input.

Parts List

Component	Quantity
Tern FlashCore-B Microcontroller	1
PIC18LF2620 Microcontroller	1
3.3V TO-92 LDO regulator LT1121CZ-3.3	1
Maxim 3223ECWP RS232 line driver	2
Samtec 2x4 0.05" ribbon cable	1
Trimble Lassen SQ	1
Trimble embedded antenna	1
Trimble magnetic antenna	1
Trimble antenna impedance matching cable	1
ADXL311 accelerometers	2
SHT11 Temperature and Humidity Sensor	1
Dual LED 7-segment display	1
74LVT125DR Quad Bus Buffer	4
PIC12F683 CMOS Buffer	1
ZVP2106A PFET	2
74LS32N	1
74LS08N	1
74LS151 multiplexer	1
Coin cell battery holder	1
Lithium coin cell battery	1
6V lead-acid battery	1
Inline fuse, 2A slow-blow	1
0.1uF monolithic capacitors	9
2.2uF solid tantalum capacitors	2
3.3uF tantalum capacitor	1
4700uF 10V electrolytic capacitor	1
100uF 16V electrolytic capacitor	1
110 ohm resistor	1
150 ohm resistor	4
100 k ohm resistor	4
120 k ohm resistor	2
Transistor sockets	3
14-pin solder-tab IC sockets	2
2x10-pin female header	1
2"x3" solder-pad perfboard	1
2x10-pin male header	1
20-pin wire-wrap IC sockets	2
32-pin wide wire-wrap IC socket	1
20-pin wire-wrap IC sockets	2
14-pin wire-wrap IC sockets	3
2x10-pin male header	4
2x8-pin male header	1
Plastic 4-40 washers	4
4-40 nuts	2
4-40 washers	2
2x5-pin male headers	2
2x4-pin male header	1
30-pin female socket	1
4-pin female socket	1
Breakaway header, 100mils	1
PS/2 cable	1

APPENDIX B : 125 KHZ INDUCTIVE LINK SCHEMATICS

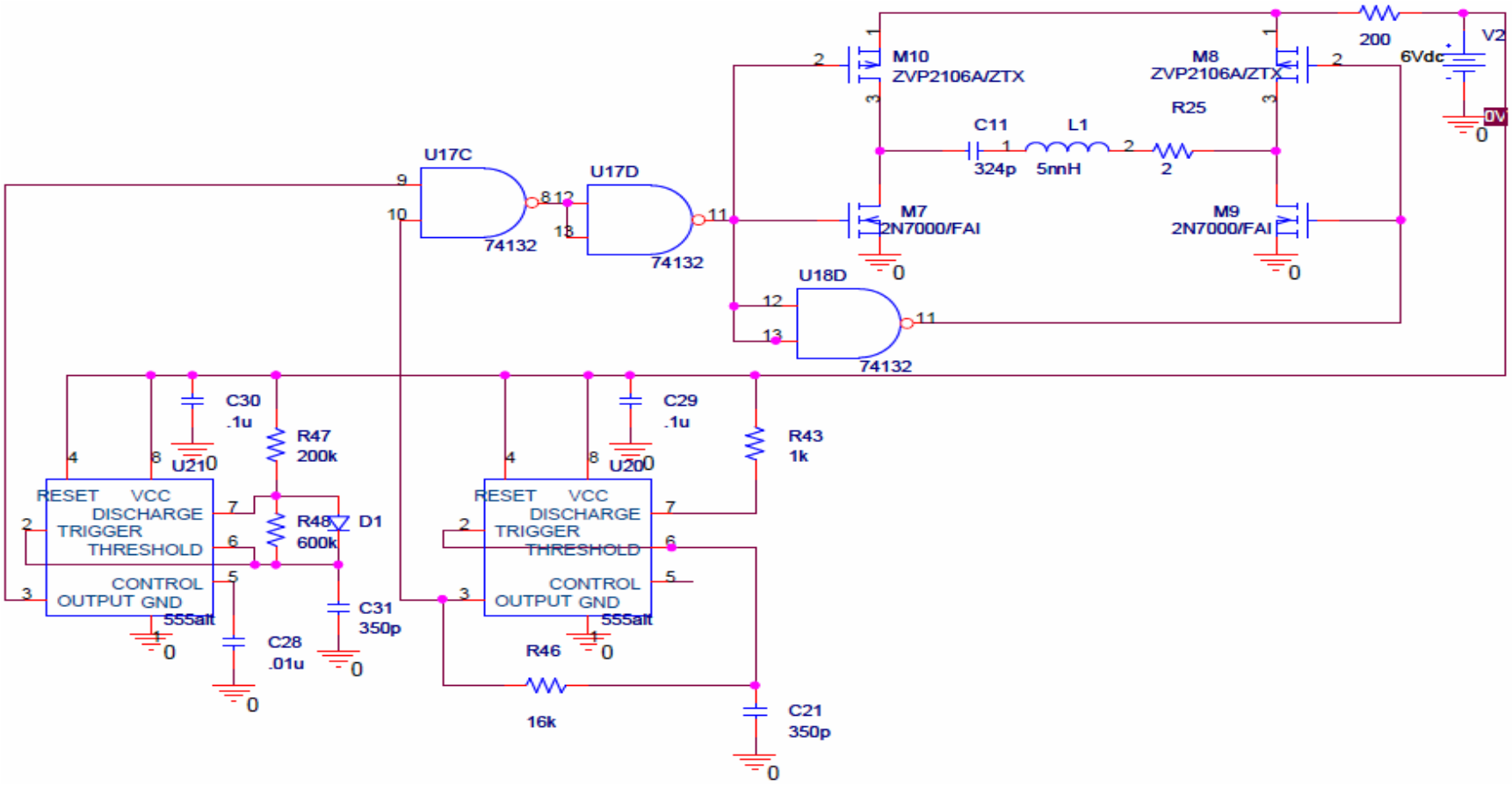

Figure 22. 125 kHz inductive transmitter schematics.

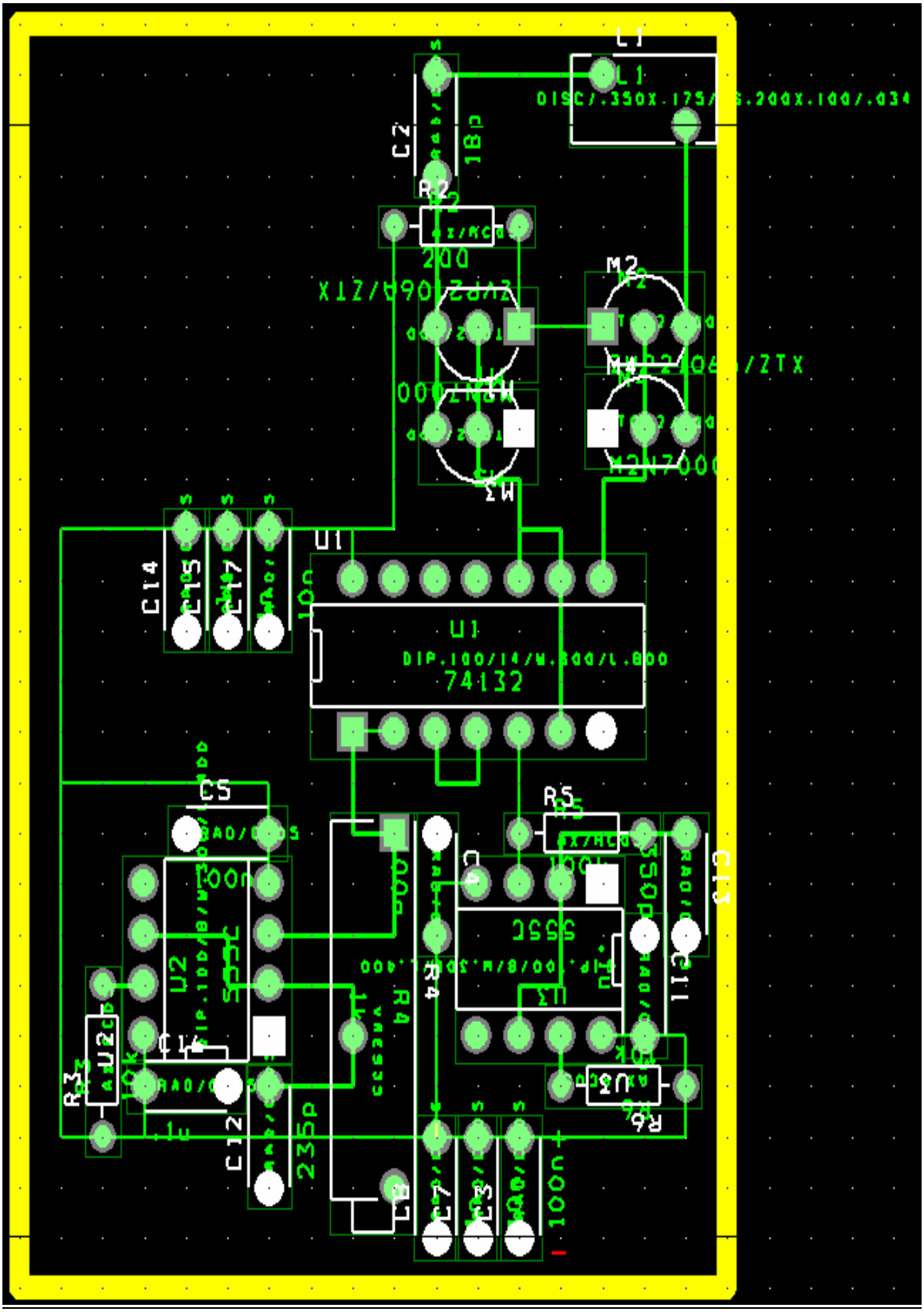

Figure 23. 125 kHz inductive transmitter protoboard layout.

Parts List

Component	Quantity
74LS132 Quad 2-Input Schmidt NAND Gate	1
LMC555 CMOS Timer	2
ZVP2106 (or equivalent) P-Channel MOSFET	2
2N7000 (or equivalent) N-Channel MOSFET	2
Custom Wrapped 5mH Inductor	1
324pF ceramic capacitor	1
1-5pF trimcap capacitor	1
0.01 uF electrolytic capacitor (decoupling)	3+
0.1 uF tantalum capacitor (decoupling)	3+
0.1 uF mica capacitor (decoupling)	3+
350 pF ceramic capacitor	2
Rectifier Diode	1
200 Ohm ceramic resistor	1
1 k Ohm ceramic resistor	1
16 k Ohm ceramic resistor	1
200 k Ohm ceramic resistor	1
600 k Ohm ceramic resistor	1
324pF ceramic capacitor	1
AA battery (1.5v)	4
Quad-AA battery connector with 4 pin output	1

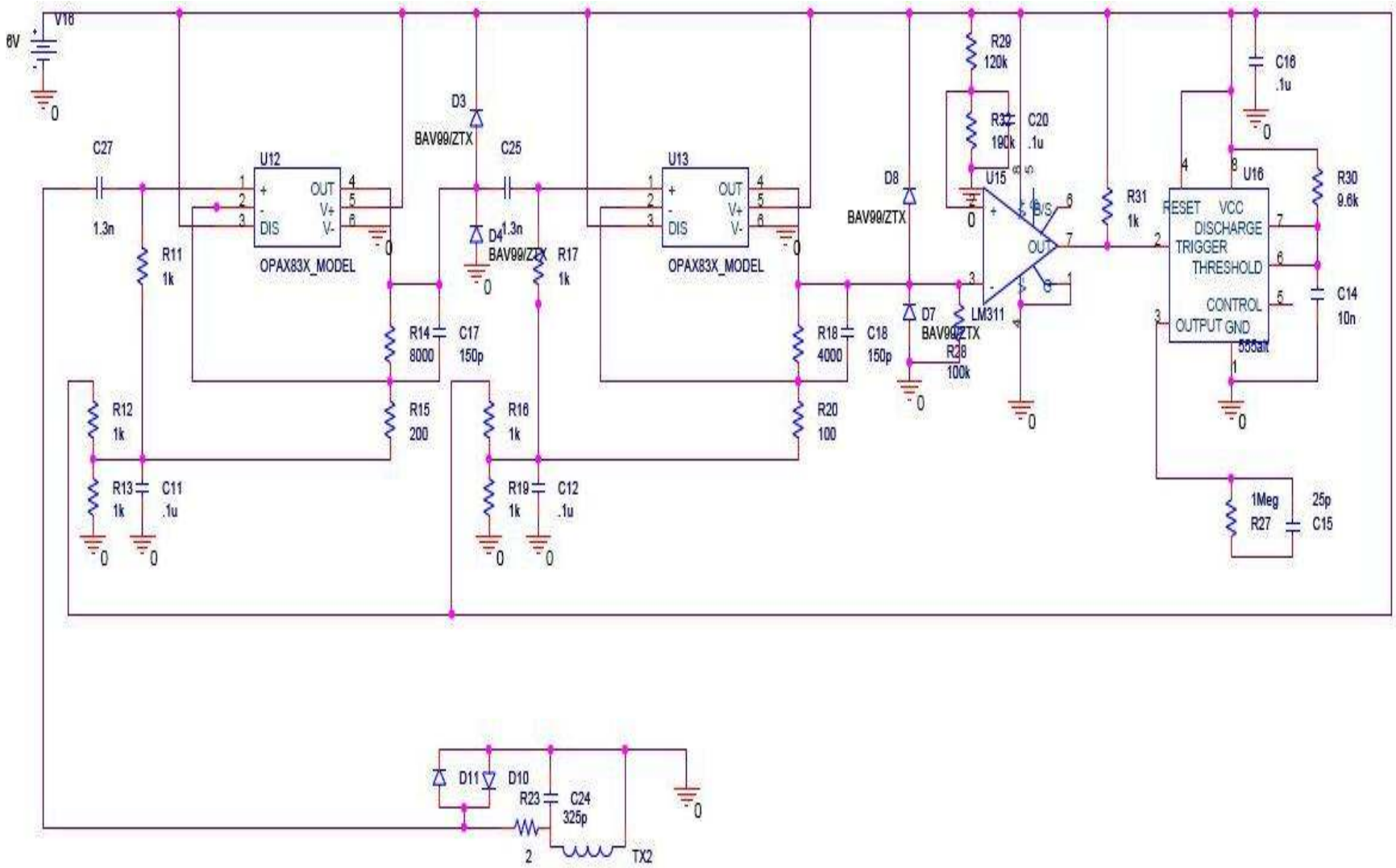

Figure 24. 125 kHz inductive receiver schematics.

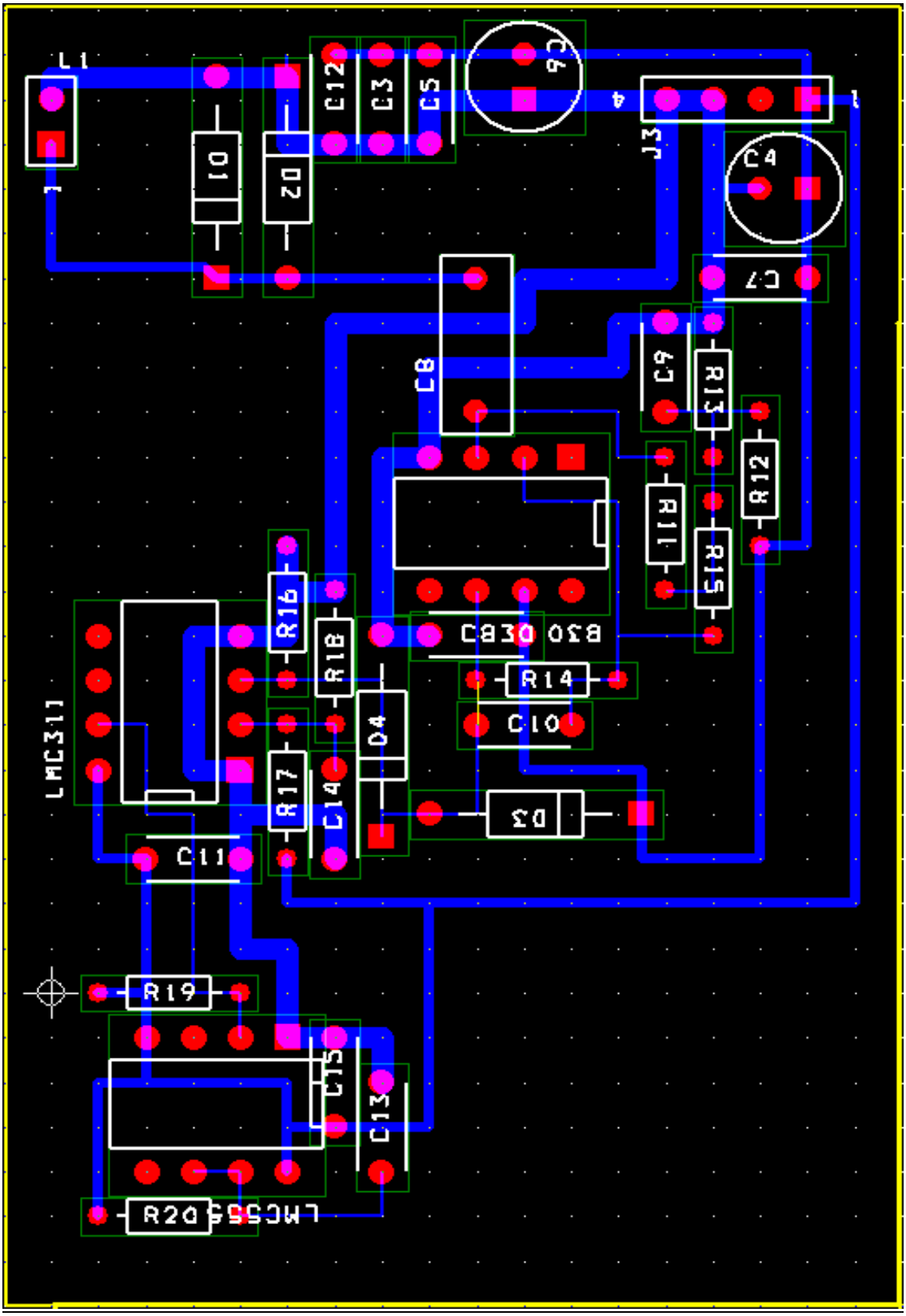

Figure 25. 125 kHz inductive receiver protoboard layout.

Parts List

Component	Quantity
OPA830 Dual Operational Amplifier	1
LM311 Voltage Comparator	1
LMC555 CMOS Timer	1
Custom Wrapped 5mH Inductor	1
324pF ceramic capacitor	1
1-5pF trimcap capacitor	1
0.01 uF electrolytic capacitor (decoupling)	4+
0.1 uF tantalum capacitor (decoupling)	4+
0.1 uF mica capacitor (decoupling)	4+
350 pF ceramic capacitor	2
1.3 nF ceramic capacitor	2
10 nf ceramic capacitor	1
Rectifier Diode	6
100 Ohm ceramic resistor	1
200 Ohm ceramic resistor	1
1 k Ohm ceramic resistor	7
4 k Ohm ceramic resistor	1
8 k Ohm ceramic resistor	1
9.6 k Ohm ceramic resistor	1
100k Ohm ceramic resistor	1
120k Ohm ceramic resistor	1
190k Ohm ceramic resistor	1
AA battery (1.5v)	4
Quad-AA battery connector with 4 pin output	1